LAJSBA
LATIN AMERICAN JOURNAL OF SEDIMENTOLOGY AND BASIN ANALYSIS | VOLUME 25 (2) 2018, 117-148

PALEOSOLS AND RELATED SOIL-BIOTA OF THE EARLY MIOCENE SANTA CRUZ FORMATION (AUSTRAL-MAGALLANES BASIN, ARGENTINA): A MULTIDISCIPLINARY APPROACH TO RECONSTRUCTING ANCIENT TERRESTRIAL LANDSCAPES

M. Sol Raigemborn [1,2,], Verónica Krapovickas [3], Alejandro F. Zucol [4], Luciano Zapata [5], Elisa Beilinson [1,6], Nestor Toledo [7], Jonathan Perry [8], Sabrina Lizzoli [1], Lucía Martegani [9], David E. Tineo [1,10], Esteban Passeggi [4]*

[1] CONICET - UNLP. Centro de Investigaciones Geológicas, Diagonal 113 Nº 275 (1900) La Plata, Argentina.
[2] Cátedra de Micromorfología de Suelos, Facultad de Ciencias Naturales y Museo, UNLP, Calle 122 y 60 s/n, (1900) La Plata, Argentina.
[3] IDEAN - CONICET, Departamento de Ciencias Geológicas, FCEyN, UBA, Ciudad Universitaria, Pab. 2, (C1428EHA) Buenos Aires, Argentina.
[4] Laboratorio de Paleobotánica, Centro de Investigaciones Científicas y Transferencia de Tecnología a la Producción (CICYTTP-UADER Provincia de Entre Ríos - CONICET), Dr. Materi y España SN, E3105BWA, Diamante, Argentina.
[5] Cátedra de Fundamentos de Geología, Facultad de Ciencias Naturales y Museo, UNLP, Calle 122 y 60 s/n (1900) La Plata, Argentina.
[6] Cátedra de Sedimentología Especial, Facultad de Ciencias Naturales y Museo, UNLP, Calle 122 y 60 s/n (1900) La Plata, Argentina.
[7] División Paleontología Vertebrados, Unidades de Investigación, Anexo Museo, Facultad de Ciencias Naturales y Museo, Avenida 60 y 122, 1900, La Plata, Argentina. CONICET.
[8] Center for Functional Anatomy and Evolution, The Johns Hopkins University School of Medicine, Baltimore, USA.
[9] Cátedra de Mineralogía, Facultad de Ciencias Naturales y Museo, UNLP, Calle 122 y 60 s/n (1900) La Plata, Argentina.
[10] Cátedra de Geología de Combustibles, Facultad de Ciencias Naturales y Museo, UNLP, Calle 122 y 60 s/n (1900) La Plata, Argentina.
* msol@cig.museo.unlp.edu.ar

ARTICLE INFO

Article history
Received December 10, 2018
Accepted June 8, 2019
Available online June 10, 2019

Invited Editor
José I. Cuitiño

Handling Editor
Sebastian Richiano

Keywords
Pedotypes
Ichnofossils
Phytoliths
Vertebrates
Santa Cruz Province

ABSTRACT

The middle and upper parts of the lower Miocene Santa Cruz Formation (~17–15.9 Ma) in the southeastern Austral-Magallanes Basin (southern Patagonia, Argentina) crop out as a fluvial succession that in parts is pedogenically modified. The study of the paleosols of this unit combined with the study of ichnofossils, microremains, and fossil vertebrates present in these allows us to reconstruct past environmental, ecological, and climatic conditions, as well as paleolandscape evolution of the Santa Cruz Formation during ~1 my. These reconstructions demonstrate three different stages during which very weak to moderate pedogenesis took place. The first one (middle part of the unit) is an epiclastic distal floodplain bearing Calcisols or paleo-calcic Inceptisols, which record a relatively dense vegetation integrating trees, shrubs, palms, and short grasses. Soil fauna is scarce and it is in association with a vertebrate fauna typical of coastal "Santacrucian assemblages". The second landscape stage (the bottom of the lowermost upper part of the unit) is composed of epiclastic distal floodplain areas and minor pyroclastic proximal floodplain settings that contain mainly Vertisols. Vertisols record an ecosystem dominated by grasses and palms adapted to variable conditions in hydric availability (C_4 plants) and by solitary bee larvae, and adult and nymph soil beetles. Finally, up-section, the third stage attests to the existence of an epiclastic and pyroclastic distal and proximal floodplain over which Protosols developed. Past ecosystems supported grass vegetation (C_3 plants), oligochaete annelids and a moderately diverse insect soil fauna (interpreted by their trace fossils) composed of solitary bee larvae, soil beetles and their pupae, cicada nymphs, and myriapods. This combined abiotic (paleosols) and biotic (ichnofossils, microremains, and vertebrates) study indicates

that several factors controlled the landscape evolution during the early Miocene of southeastern Patagonia. Highly aggrading fluvial conditions, variations in the position in the floodplain and in sedimentation/pedogenesis ratio, the input of pyroclastic materials, the length of landscape stability, changing hydrologic conditions, and fluctuations of wetter and drier phases in a context of relatively warm and humid climate, seem to be the main factors controlling the landscape.

INTRODUCTION

Paleosols and their constituents, including ichnofossils and microremains such as phytoliths, together with the fossil fauna preserved in these soils, can be helpful tools to interpret paleoenvironmental, paleoecological, and paleoclimatic conditions in continental settings (*e.g.*, Kraus and Hasiotis, 2006; Sheldon and Tabor, 2009; Hembree and Bowen, 2017). This is because the soil development is influenced, among other things, by environmental factors such as climate and organisms (*e.g.*, Retallack, 2001; Buol *et al.*, 2011). At the same time, as ichnofossils (structures biologically produced *in situ* that result from the movement of organisms through or on a medium) respond directly to the environment in which they formed, they can be thought of as representatives of the environments in which they are preserved (Bromley, 1996). Similarly, phytoliths (microscopic silica particles formed inside living plants) preserved within paleosols provide the record of vegetation composition and allow ecosystem reconstructions (*e.g.*, Zucol *et al.*, 2018). In addition, the analysis of vertebrate fauna from paleosols leads to the understanding of paleoecological conditions (*e.g.*, presence of taxa adapted to open and arid environments or adapted to vegetated and humid ones). Thus, the association of paleosols, ichnofossils, and phytoliths —together with fossil mammals— provide direct and complementary evidence of ancient terrestrial landscapes from both biotic and abiotic perspectives (*e.g.*, Retallack, 2001; Kraus and Hasiotis, 2006; Hasiotis and Platt, 2012; Kohn *et al.*, 2015; Catena *et al.*, 2016, 2017; Hembree and Bowen, 2017; Badawy, 2017).

The Santa Cruz Formation (SCF) is an upper lower Miocene unit of estuarine to fluvial origin that crops out widely in the Austral-Magallanes Basin (southern Patagonia, Argentina) (*e.g.*, Raigemborn *et al.*, 2015; Cuitiño *et al.*, 2016a). The SCF has been widely studied since the 19th Century due to the richness in fossil mammals (Santacrucian South American Land Mammal Age) (see Vizcaíno *et al.*, 2012 for a review). These paleontological (faunal and vegetational) studies and their paleoenvironmental reconstructions were mainly constrained to the lower part of the unit, which crops out along the Atlantic coastal cliffs in southern Santa Cruz Province (Fig. 1A) (*e.g.*, Tauber, 1994, 1997a, 1997b; Kay *et al.*, 2008, 2012; Brea *et al.*, 2012, 2017; Zucol *et al.*, 2015; Crifò *et al.*, 2016, 2017, 2018). In the last few years, environmental reconstructions based on sedimentological and ichnological analysis of the entire unit have been published (Krapovickas, 2012; Matheos and Raigemborn, 2012; Raigemborn *et al.*, 2015; Cuitiño *et al.*, 2016b, Zapata *et al.*, 2016; Zapata, 2018). These studies have highlighted the occurrence of subtropical environments with a vegetation mosaic of open and closed habitats that occupied fluvial environments. Meanwhile, the middle and upper parts of the unit seem to record the existence of environments adapted to more arid and seasonal conditions than those prevailing during the deposition of the lower part of the SCF. However, pedological, ichnological, and phytolithic analyses of the SCF in the southernmost part of Santa Cruz Province, and past environmental reconstructions based on these studies are still very scarce (Krapovickas, 2012; Zapata *et al.*, 2016; Raigemborn *et al.*, 2018a). Similarly, with the exception of Tauber´s work (see above), Santacrucian fossil faunas in this area of the basin have never been studied in detail. Therefore, a combined paleopedological, ichnological, and paleobotanical analysis of the SCF, supported by paleontological studies, represents a potential archive of data to complement previous environmental interpretations and allows us to test changing terrestrial conditions. This contribution interprets the early Miocene environments in the south of the Santa Cruz Province (Austral-Magallanes Basin) and reconstructs terrestrial landscapes based on an integrated abiotic-biotic study of the middle and upper parts of the SCF.

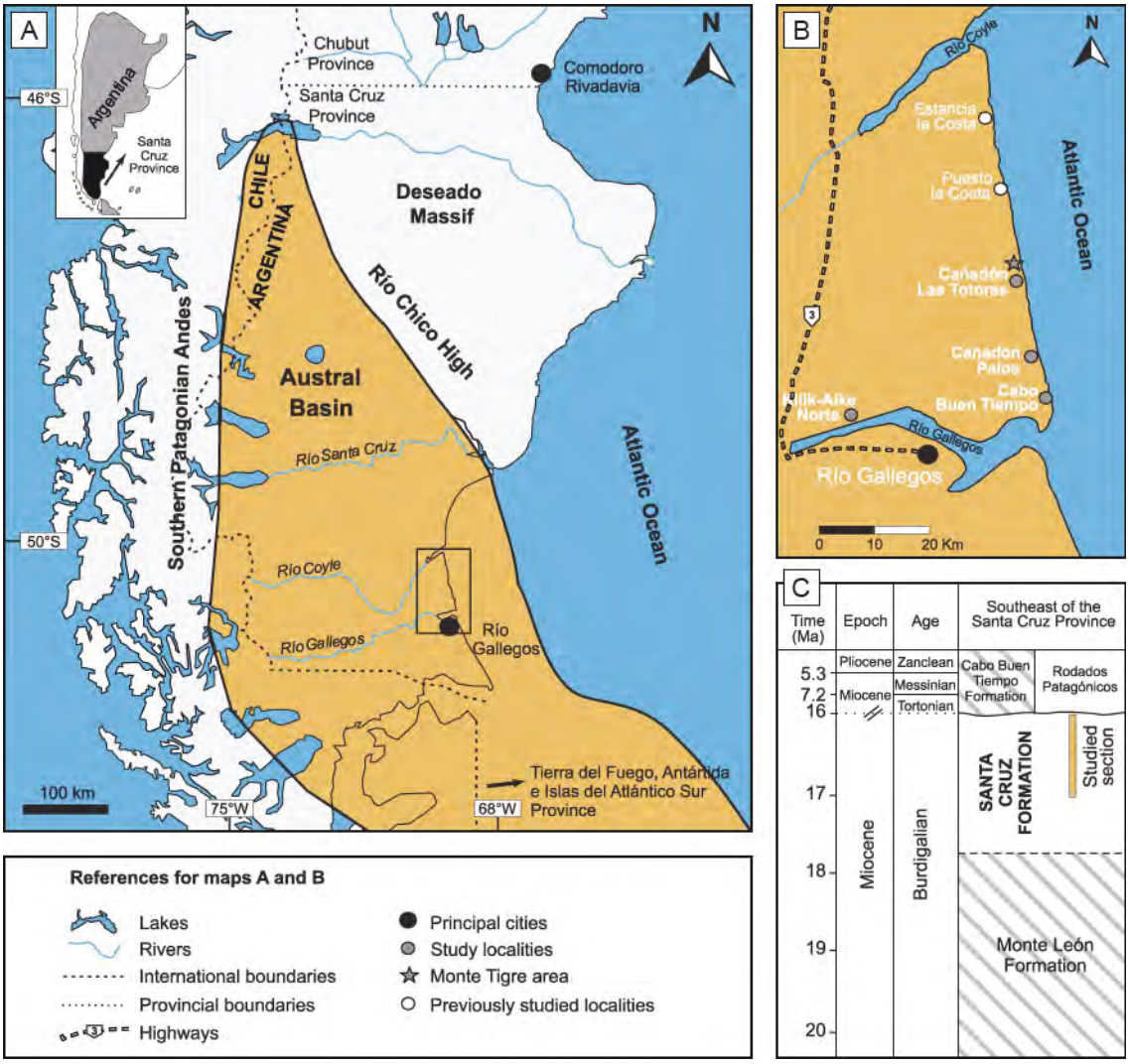

Figure 1. a) Map showing position and boundaries of the Austral-Magallanes Basin (after Biddle *et al.*, 1986), and position of the study localities (rectangle). **b)** Location of the analyzed sections of the Santa Cruz Formation and previously studied ones. **c)** Stratigraphic chart of the southeast Santa Cruz province with the position of the studied interval (modified from Raigemborn *et al.*, 2018a). It extends through continental (white) and marine (striped) units.

GEOLOGICAL AND SEDIMENTOLOGICAL BACKGROUND

The Austral-Magallanes Basin is located in southernmost South America (Fig. 1A–B). During its foreland stage (Cretaceous and Cenozoic), the basin was infilled with marine sediments deposited during several Atlantic transgressions that were intercalated with intervals of non-deposition, erosion, and continental deposition (Biddle *et al.*, 1986; Malumián, 1999). In particular, during the lower Miocene the basin was infilled with the marine deposits of the Monte Léon Formation (Bertels, 1970) and equivalent units, which were transitionally succeeded by the early Miocene estuarine and fluvial deposits of the SCF (Matheos and Raigemborn, 2012; Raigemborn *et al.*, 2015). The upper Miocene–Pleistocene marine and glaciofluvial sediments of the Cabo Buen Tiempo Formation (Hatcher, 1897) and the "Rodados Patagónicos" (Fidalgo and Riggi, 1970) (Fig. 1C) disconformably overlie the SCF. The SCF in the Atlantic coastal cliffs of southern Santa Cruz Province (Fig. 1B) is a ~225 m-thick succession composed mainly of stacked fluvio/alluvial deposits intercalated with paleosols (Genise and Bown, 1994; Tauber, 1994; Matheos and Raigemborn, 2012; Raigemborn *et al.*, 2015; Zapata *et al.*, 2016; Zapata, 2018). In the lower part of the unit an estuarine environment was formed

(Raigemborn *et al.*, 2015; Cuitiño *et al.*, 2016a; Parras and Cuitiño, this volume). Tauber (1994, 1997a, 1997b) divided the SCF into two members based on lithological aspects, separated by a locally erosional discontinuity: the lower Estancia La Costa Member, dominated by pyroclastic and epiclastic mudrocks, and the upper Estancia La Angelina Member, dominated by epiclastic muddy and sandy deposits. Recently, sedimentological analysis of the Atlantic SCF south of Río Coyle, allowed Zapata (2018) to differentiated five sections: I, II, III, IV, and V (see below). Sections I–III correspond to the Estancia La Costa Member; meanwhile sections IV–V are equivalent to the Estancia La Angelina Member.

In the study area (Cañadón Las Totoras, Cañadón Palos, Cabo Buen Tiempo, and Killik-Aike Norte localities, Fig. 1B), the SCF outcrops are 15–90 m thick and are exposed mainly along the sea cliffs. The outcrops of the SCF studied in this contribution correspond to the middle part of the unit (*i.e.,* the upper part of the Estancia La Costa Member, or section III of Zapata, 2018), and to the upper part of the unit (*i.e.,* the Estancia La Angelina Member, or sections IV and V). Middle and upper parts of the SCF range in age from ~ 17.0 to 15.9 Ma (Perkins *et al.*, 2012; Fig. 1C). In these studied localities, the base of the SCF is not exposed and its top is truncated by the "Rodados Patagónicos" or by the Cabo Buen Tiempo Formation (Figs. 1C and 2).

According to Zapata (2018), sections III, IV and V of the SCF are predominantly made up by floodplain deposits frequently affected by pedogenesis. These deposits show a distinct lithological change between section III and sections IV–V, from epiclastic (Sm, Fm and Fl facies) to pyroclastic with varying degrees of epiclastic participation (Tm, Tr, Sm, Fm and Fl facies; see Table 1 and Fig. 2). Zapata (2018) also characterized the fluvial channel styles that develop in each section, all of which are composed by coarse-grained beds (Gt, St and Sp facies; see Table 1 and Fig. 2) regardless of their stratigraphic location. Even though all the studied sections of the SCF correspond to moderate–high energy fluvial systems, important geometric and architectural differences can be distinguished between them. Section III channels show broad ribbon and narrow sheet-like morphologies, interpreted as confined and unconfined simple channels. Section IV channels can be described as narrow and broad ribbons, and narrow sheets interpreted mainly as confined simple channels, and in less proportion as unconfined simples and confined complex channels. Section V channels show broad and narrow ribbon-like morphologies, and were interpreted as confined, laterally stable, simple channels by Zapata (2018).

METHODS AND SAMPLES

Ichnofossils and the paleosols that contain them were sampled in the study area at the four localities mentioned before. Paleosols were identified in outcrop based on macroscopic pedofeatures such as structure, mottles, nodules, color, slickensides, as well as rhizoliths and other trace fossils (*e.g.*, Retallack, 2001) (Fig. 2). For each paleosol horizon, thickness, contact types, mineral composition, mean grain size, ped structure, type of nodules, and evidence of bioturbation were described (*e.g.,* Retallack, 2001; Schoeneberger *et al.,* 2012). Colors were described according to the Munsell notation (Munsell Soil Color Book, 2013). Additionally, a micromorphological analysis was also undertaken. Thin sections of paleosol matrix were studied in order to establish mean grain size, mineralogical composition, porosity, microstructure, pedofeatures, fine material (groundmass), and microfabrics. Here we applied the criteria of Bullock *et al.* (1985), Stoops (2003), and Stoops *et al.* (2010). Selected paleosols were collected to determine clay composition. Clay mineralogy was determined from X-ray diffraction (XRD) pattern. The methodology used for sample preparation and semi-quantification of the minerals follows Raigemborn *et al.* (2014). Analyses were run on a PANalytical X´Pert PRO diffractometer (Centro de Investigaciones Geológicas, La Plata, Argentina), using Cu radiation (Kα = 1.5 Å) and a Ni filter, with generation settings of 40 kV and 40 mA. Routine air-dried mounts were run between 2 and 32 °2θ at a scan speed of 2 °2θ/min. Samples were ethylene glycol-solvated without saturation pre-treatment and heated to 550 °C. Then they were run from 2 to 27 °2θ and 3 to 15 °2θ, respectively, at a scan speed of 2 °2θ /min. Paleosol classification was based on macro- and micromorphological features recognized in the constituent horizons, and on mineralogical analysis (XRD) through a comparison with the USDA (United State Department of Agriculture) soil taxonomy (Soil Survey Staff, 1999; Schoeneberger *et al.*, 2012) and with the paleosol classification of Mack *et al.* (1993).

The trace fossils studied are mostly preserved

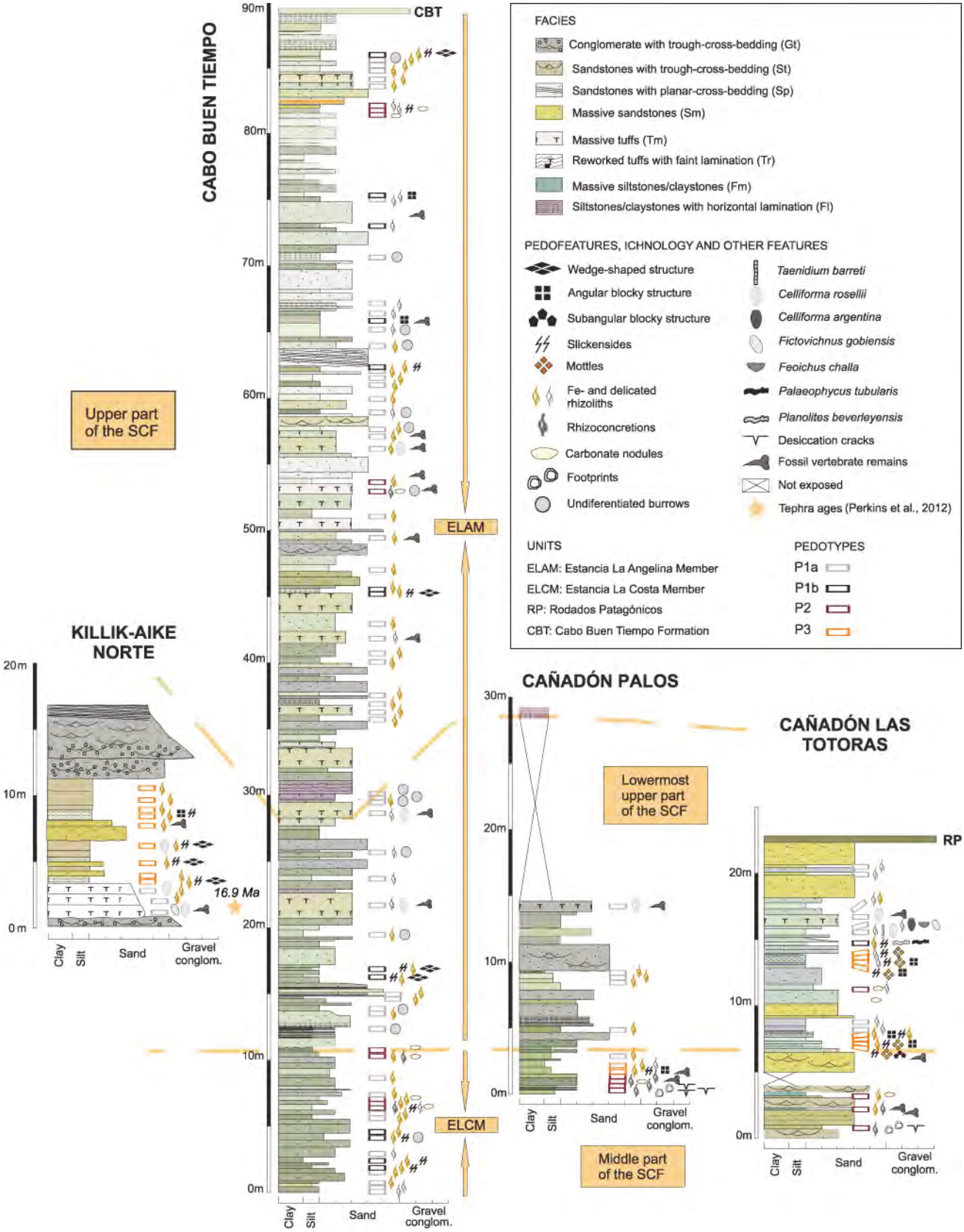

Figure 2. Measured sedimentary sections including facies, pedotypes, and the stratigraphic intervals of the Santa Cruz Formation defined by Zapata (2018). Note that the middle part of the SCF is equivalent to the uppermost part of the Estancia La Costa Member of Tauber (1994, 1997a, 1997b), and that the lowermost upper part and the upper part of the SCF correspond to the Estancia La Angelina Member of Tauber (1994, 1997a, 1997b).

Facies code	Features	Interpretation	Associated pedotypes
Gt, St, Sp	Fine-grained conglomerate to medium-grained sandstones with trough/planar cross-bedding.	Simple and complex (confined an uncofined) channel	-
Sm	Medium–very fine massiv sandstones	Non-channelized sandy sheetflood of the proximal–distal floodplai	P1a, P1b, P2, P3
Tr	Medium–fine reworked tuffs wi faint lamination	Unconfined pyroclatic sheetfloods the proximal floodplai	P1a, P1b
Tm	Massive very fine tuffs	Ash-fall deposits in distal floodplai settings	P1a, P1b, P2, P3
Fm	Massive siltstones–claystones	Suspension fallout in still-stand water in the distal floodplai	P1a, P1b, P2, P3
Fl	Siltstones–claystones with horizontal lamination	Deposition from suspension and from traction currents in distal floodplain area	P1a, P1b,

Table 1. Facies scheme for the Santa Cruz Formation and associated paleosols.

in the field. The most relevant specimens were collected at the study area and stored in the Museo Regional Provincial Padre M. J. Molina (MPMPIC), Río Gallegos, Santa Cruz Province, Argentina. The material collected correspond to: 1) *Celliforma roselli* (MPM-PIc-17567; 17569–17570; 17575; 17580; 17583; 17587–17590; 17593–17594; 17597–17607; 17609– 17611); 2) *Celliforma argentina* (MPM-PIc-3632; 17566; 17568; 17571– 17574; 17577–17579; 17581–17582; 17584–17586; 17591–17592; 17595–17596); 3) *Feoichnus challa* (MPM-PIc-17614, MPM-Pic-17615); 4) *Fictovichnus gobiensis* (MPM-PIc-17612, MPM-PIc-17613); 5) MPM-PIC 3638, a delicate root trace; and 6) MPM-PIC 3640, part of the horizontal rhizoconcretions system (see Krapovickas, 2012). Rhizoliths were described and identified following Klappa (1980).

For phytolith analysis, 32 paleosol samples (each sample consisted of twenty grams of sediment) grouped according to the pedotype to which they belong were taken and processed following a protocol employing various chemical agents to remove soluble salts, organic matter, and carbonates (see Zucol *et al.*, 2010). Samples were observed in a Nikon Eclipse E200 light microscope, and microphotographs were taken with a Nikon Coolpix 990 digital camera. Based on the phytoliths found, morphotypes were counted and established based on recent contributions on woody (Mercader *et al.*, 2009; Stromberg *et al.*, 2013; Collura and Neumann, 2017) and herbaceous (Barboni and Bremond, 2009; Mercader *et al.*, 2010; Neumann *et al.*, 2017) species phytoliths. As in those studies on preserved wood, we have taken a comparative approach to establish the botanical affinity of these morphotypes and life-form of the plants in which they originated. The major groups of microremains on which we focused these studies were radiolarians, sponge spicules (whole and fragmented), charcoals, diatoms, sporomorphs, and phytoliths (considering multicellular, eroded, and unicellular phytoliths). Sedimentary samples and microscope slides are stored in the Paleobotanical Laboratory Collection of the Centro de Investigaciones Científicas de Diamante (CICYTTP–CONICET, Diamante, Argentina), under the acronyms CIDPALBO-MS 3791–3812; 3816–3825.

Fossil vertebrates were collected in Monte Tigre (a locality very close to Cañadón Las Totoras) and Cañadón Palos (see Fig. 1B) during field seasons conducted previously by colleagues (S.F. Vizcaíno, M.S. Bargo, and R.F. Kay) and by some of us (NT and JP). Collections were made with reference to fossiliferous levels as defined by Tauber (1997a), and recording coordinates, noting orientation, and taking photographs. Fossils were cataloged and housed at the permanent collections of the Museo Regional Provincial Padre M.J. Molina in the city of Río Gallegos (Santa Cruz Province).

GENERAL FEATURES OF THE PALEOSOLS OF THE SANTA CRUZ FORMATION

Paleosols of the SCF crop out in the study area as continuous tabular beds, pale greenish yellow to grayish olive in color, and defined pedogenic horizons can be recognized in them (Fig. 2). Internally, these horizons are mainly massive or they show variations in the arrangement of soils aggregates ranging from incipient to well-defined wedge-shaped to angular-subangular blocky structure (Fig. 2). In a few cases, a relict primary lamination was recognized. The most conspicuous macropedofeatures are ferric and delicate rhizoliths, and slickensides (Fig. 2). Mottles, carbonate rhizoliths, and desiccation cracks are less frequent (Fig. 2). Abundant vertebrate fossil remains also occur, as well as invertebrate and vertebrate trace fossils (Figs. 2 and 3).

ICHNOFOSSILS OF THE SANTA CRUZ FORMATION

Celliforma rosellii Genise and Bown, 1994

This trace fossil mostly comprises indurated internal molds of isolated breeding or nidification chambers (Callichnia). Cells are oval shaped, with one rounded end and one flattened end. They have a smooth lining and lack discrete walls and antechambers (Fig. 3A). The dimensions of the internal mold cell are 1.3–2.3 cm long and 0.7–1.2 cm-wide, coincident with the type material described from the same unit. Some cells record a basal area of different coloration that represents the exceptionally preserved semiliquid food provision for the developing bee larva (Fig. 3A) (Zapata *et al.*, 2016).

Celliforma argentina Zapata *et al.*, 2016

As with *C. rosellii*, *Celliforma argentina* consists of single isolated chambers in a vertical orientation without antechambers and with discrete walls (Genise, 2000; Zapata *et al.*, 2016). In particular, the *C. argentina* comprise an internal mold of barrel shape; the inferior end of the chamber is rounded to flattened. By contrast, in *C. rosellii* the inferior end of the chamber is rounded to pointed, producing an oval shape for the whole cell. In addition, in *C. argentina* the dimension of the cells is markedly smaller than in *C. rosellii*: in complete specimens of *C. argentina*, the length seldom if ever exceeds 1.1 cm (Fig. 3B). Mean length for SCF specimens of this ichnospecies is 0.9 cm and mean diameter is 0.5 cm. The difference in size between the two ichnospecies of *Celliforma* could indicate that these trace fossils were made by two different bee taxa. As the brood cells are produced by adults, it is clear that the material does not correspond to ontogenetic series. In addition, intraichnospecific size variation within *C. argentina* do not overlap with that expressed by *C. rosellii*.

Feoichnus challa Krause *et al.*, 2008

The trace fossil consists of an unfilled hemispherical, upwardly concave, dish-shaped structure attributed to a cicada nymph feeding chamber. The internal surface is smooth with irregularly distributed pits and scratches while the external surface is rough and irregular, without ornamentation (Fig. 3G). The preservation of only the base (dish-shaped structure) of the chamber results from the drainage of anal secretions held in the chamber and the impregnation of the surrounding soil particles, with pedogenic processes precluding the preservation of the rest of the chamber. Finally, the pits correspond to impression of the legs of the producer. In the best preserved specimen the external diameter is 1.4 cm, the height is 0.6 cm and the depth is 0.2 cm. The wall thickness varies at the base from 1 to 3 cm and the lateral wall is 0.3 cm thick.

Fictovichnus gobiensis Johnston *et al.*, 1996.

These trace fossils correspond to internal cast of chambers that are ellipsoid to ovoid in shape with a smooth internal surface and no wall. Both ends of the chambers are rounded and lack terminal, sub-terminal, or medial scars (Fig. 3H). They correspond to pupal chambers of beetles that pupate in the soil such as Scarabaeidae, Tenebrionidae, and Curculionidae (Johnston *et al.*, 1996). The chambers are 0.84-0.95 cm long and 0.42-0.45 cm wide. The SCF material would mainly correspond to failed cocoons as they are mostly preserved as complete chambers (Zapata *et al.*, 2016). Only two specimens were collected although many were recorded *in situ* at Killik-Aike Norte locality.

Palaeophycus tubularis Halls, 1847.

This trace fossil consists of simple dwelling bur-

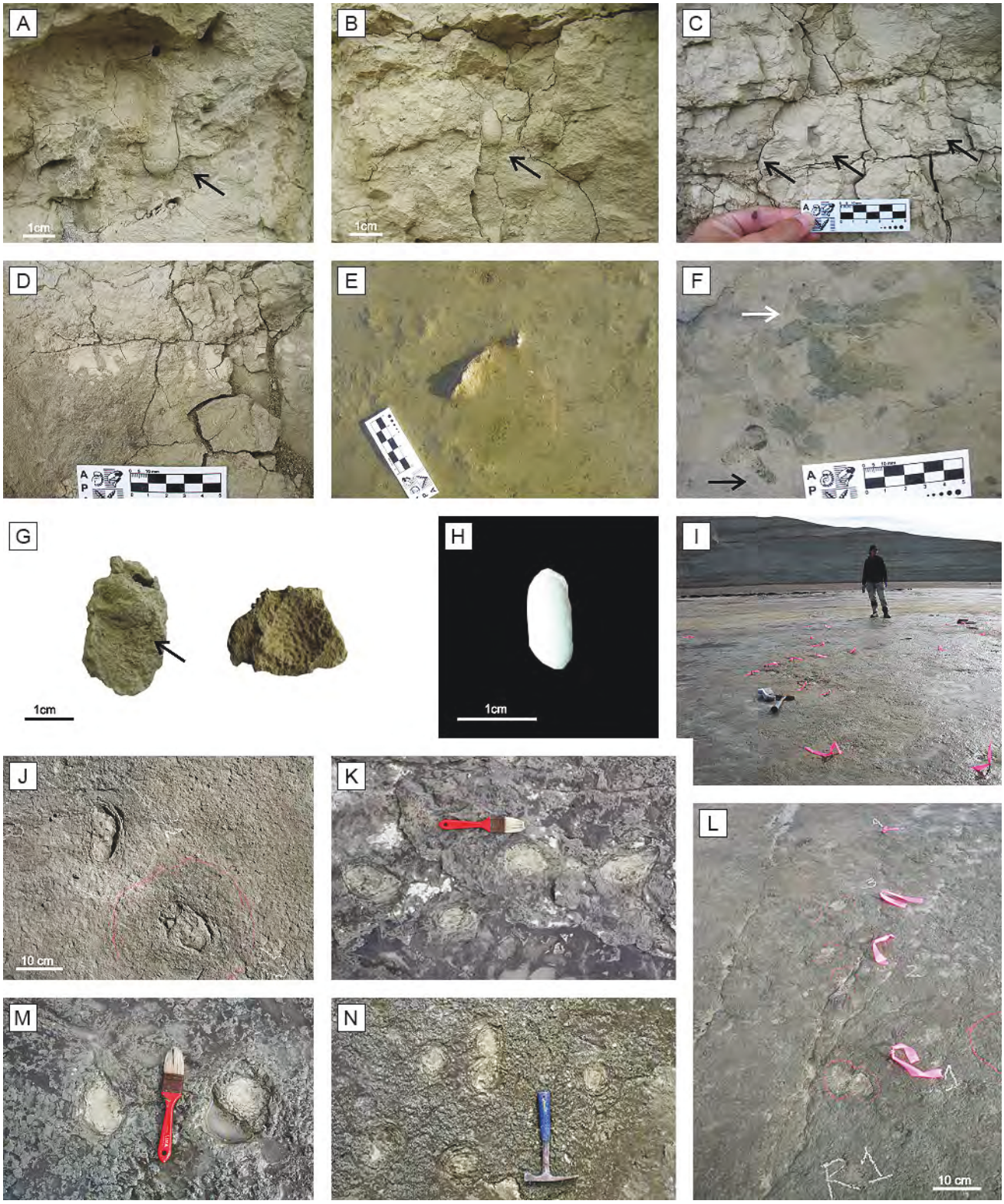

Figure 3. Invertebrate and vertebrate trace fossils of the SCF. **a)** *Celliforma rosellii.* Note a basal area of different coloration (arrow) that represents the exceptionally preserved semiliquid food provision for the developing bee larva. **b)** *Celliforma argentina* (black arrow). **c)** From left to right *C. argentina, C. rosellii,* and ferric root traces recorded at Cañadón Las Totoras. **d)** *Palaeophycus tubularis* recorded at Killik-Aike Norte. **e)** *Planolites beverleyensis* recorded north of Cañadón Las Totoras. **f)** *Taenidium barretti* (black arrow) and *Palaeophycus tubularis* (white arrow) recorded north of Cañadón Las Totoras. **g)** *Feoichnus challa,* to the right is the best preserved specimen. The arrow marks lined layers at the base of the specimen interpreted as the displacement of the feeding chamber. **h)** *Fictovichnus gobiensis* recorded at Killik-Aike Norte. **i)** Tracking surface at Cañadón las

row (Domichnia). It is sub-horizontally oriented, straight to slightly curved, with smooth walls and a thin lining (Fig. 3D and F). The burrow infill is similar to the surrounding rock, passively filled, and it is preserved as full relief or as a convex epirelief. Diameters range from 0.4 cm to 1.4 cm. The ichnogenus *Palaeophycus* Hall, 1847 was originally interpreted (*e.g.*, Frey *et al.*,1984; Pemberton and Frey, 1982) as produced by a worm-like trace maker, although horizontal subsuperficial burrows on recent floodplains are also produced by semi-aquatic insects including orthopterans (Tridactylidae), hemipterans (Salidae), coleopterans (Heteroceridae), and terrestrial coleopterans (Cicindelinae) (Ratcliffe and Fagerstrom, 1980; Krapovickas *et al.*, 2008). *Palaeophycus* traces are abundant in the SCF and constitute the majority of the identifiable traces of background bioturbation.

***Planolites beverleyensis* (Billings, 1862).**

This trace consists of straight to slightly curved feeding burrows (Fodinichnia), with unlined walls and sub-horizontal disposition (Fig. 3E). The infilling is without structure and different in color from the host sediment but is of the same grain size. The specimens preserved are scarce. Their diameter ranges from 0.5 to 0.8 cm. The infilling of *Planolites* Nicholson, 1873 represents sediment that was processed by the trace maker; suspected trace makers include oligochaete annelids, terrestrial insects, and millipedes (Pemberton and Frey, 1982; Hembree and Hasiotis, 2007).

***Taenidium barretti* (Bradshaw, 1981).**

These traces consist of straight to sinuous simple feeding or dwelling burrows (Fodinichnia/ Domichnia) characterized by a thinly segmented meniscate backfill and having no lining (Fig. 3F). The menisci are of alternating grain size, subtly arcuate, and 0.1 to 0.2 cm thick. Traces are preserved as full relief. Frequently, different specimens cross each another, giving a false impression that they are branching. The diameter of the traces ranges from 0.6 cm to 1.3 cm and is mostly coincident with the recorded size range of the specimens of *Palaeophycus tubularis*. That fact, together with its close spatial relationship, suggests a common producer for *Palaeophycus* and *Taenidium*.

The ethology and mode of life of the producers of *Taenidium* and other meniscate traces is contentious. Frey *et al.* (1984) originally interpreted the trace maker of *Taenidium* as a deposit feeder and oligochaete annelids as one of the possible *Taenidium* trace makers. However, arthropods tend to backfill their burrows mechanically, rather than deposit feeding. Recent and fossil animals that produce meniscate traces include terrestrial myriapods and insects like tiger beetles, crane-fly larvae, burrower bugs, cicada nymphs, and coleopteran larvae. Adults and larvae of burrowing ground beetles and scarab beetles may also produce meniscate traces (Frey *et al.*, 1984; Counts and Hasiotis, 2009; Krapovickas *et al.*, 2009).

Mammalian tracks

The SCF mammalian footprints consist of numerous isolated footprints in a trampling area without apparent trackway patterns in most cases (Krapovickas *et al.*, 2013). The footprints are true tracks, that is, natural impressions left by the foot of the animal in movement. The tracks have an outline well delineated by crests but lack morphological details such as digit impressions and plantar pads. They are filled by sediment similar to the host rock (Fig. 3I–N). Even though certain morphological details cannot be observed, it is possible to differentiate morphological groups through the analysis of contour and relative size. They are: 1) large kidney-like footprints approximately 20 cm long and 11 cm wide; 2) large sub-circular footprints approximately 16 cm long and 14 cm wide; 3) kidney- like footprints

Totoras. Note pink flags pointing out individual tracks. **j)** Large kidney-like footprints most likely produced by Megatherioidea or Mylodontidae (1). **k)** Medium sized kidney-like footprints most likely produced by Megatherioidea or Mylodontidae (3). **l)** Small sub-oval footprints, possibly produced by protherotherids (5). **m)** Large sub-circular footprints possibly produced by macrauchenids, toxodontids, or gliptodonts (2). **n)** Small sub-circular footprints possibly produced by typotherid notoungulates (6). In c), d), e) and f), the scale is in centimeters. In k) and m), the plane is 15 cm-long; in n) the pick is 28 cm-long. In j)–n), the 1–6 numbers are coincident with the mammalian track description section.

with a tapered anterior margin, roughly 15 cm long and 10 cm wide; 4) medium circles approximately 8 cm in diameter; 5) small sub-oval footprints, 6 cm long and 5 cm wide; 6) small sub-circular footprints, 5 cm in diameter (Krapovickas *et al.*, 2013). These morphological characteristics, together with a very well-known mammalian fauna, permit reasonable inferences about the producers of the traces. In the case of 1 and 3, the producer could be assigned to terrestrial ground sloths such as Megatherioidea or Mylodontidae (Xenartha, Folivora). This is mostly based on the presence of a (presumably medial) concave curvature associated with the lateral rotation of the foot (Krapovickas *et al.*, 2009). Large sub-circular footprints (2) have a size range and outline that could correspond to macrauchenids, toxodontids, and gliptodonts. The medium circular footprints (4) were assigned to medium sized toxodontids (Krapovickas *et al.*, 2013). Small sub-oval footprints (5) are comparable with those produced by protherotherids (Krapovickas *et al.*, 2009). Finally, small sub-circular footprints (6) have a size range comparable with those of typotherid notoungulates.

Root traces

A variety of root traces (rhizoliths *sens*u Klappa, 1980) is preserved in the analyzed SCF. They include, following Krapovickas (2012), mainly (1) delicate root traces, (2) ferric root traces, (3) haloed root traces, and (4) calcareous rhizoconcretions.

Delicate or filamentous root traces are 0.05–0.3 cm in diameter. They taper downwards and lack infill, probably owing to selective erosion of the infilling material. Ferric root traces have a red to yellow-brown color within the root infill and on its margins (Fig. 3C). The red and yellow-brown colors result from a mixture of iron oxides (hematite and goethite). A redder color indicates more hematite (*e.g.*, Schwertmann and Taylor, 1977; Kraus and Hasiotis, 2006). Ferric root traces vary from delicate or filamentous to those with greater size and diverse branching pattern. Some consist of vertical primary roots that taper downwards (0.5–0.2 cm wide) and have secondary roots (0.1–0.2 cm wide) that branch downwards with an inclination of 45 degrees. Others, have an almost constant diameter subtly tapering downwards from 0.7 to 0.4 cm with horizontally inclined secondary root traces. Haloed root traces represent delicate rhizoliths with drab haloes extending out into the paleosol matrix (Fig. 3C). Carbonatic rhizoconcretions are mainly vertically disposed tubular structures that comprise concentric layers of carbonate deposited on the ancient root margins (rhizosphere), with a central hole filled by the host sediment, where the ancient root was located (Raigemborn *et al.*, 2018a).

PALEOSOL TYPES OF THE SANTA CRUZ FORMATION

From a total of 116 pedogenically modified beds recognized through the analyzed profiles of the SCF in the study area, three paleosol types (pedotypes) were defined (Figs. 2, 4, 5 and 6; and Table 2). Surface A horizons, where paleosols were not removed by erosion, are recognized in bioturbated beds. The subsurface Bk horizons are defined by how they reflect the concentration of pedogenic carbonate (rhizoconcretions and/or nodules). The Bss designation represents a horizon that has abundant slickensides. Basal C or R horizons are assigned based on having little (C) or no (R) alteration by soil forming processes. A/C horizons are defined based on the occurrence of bioturbation and relict primary structures. As these properties are typical of both A and C horizons, an A/C horizon represents the combination of an A-type horizon and a C-type horizon (following Buol *et al.*, 2011). Similarly, B/C horizons are composed of beds that contain features of B horizons (slickensides, rhizoliths, fossil traces, incipient soil structure) and preserve characteristics of C horizons (massive or having some primary sedimentary structures).

Pedotype 1 (P1a and P1b)

This paleosol type (n=80) is widely represented (69% of all paleosols in the measured sections) in the SCF at the four studied localities (Fig. 2). P1 is developed over light gray (N7), yellowish gray (5GY 7/2), grayish yellow green (5GY 7/2), to pale olive (10Y 6/2) massive silty–clayey facies (Fm) that rarely contain primary sedimentary structures in the form of millimeter-scale planar lamination (Fl facies), massive sandstones (Sm facies), massive tuffs (Tm facies), and tuffs with relict ripples (Tr facies) (Table 1; Figs. 2 and 4). It is characterized as a grayish–greenish paleosol with very weak to weak horizonation with A/C-R (Pedotype 1a; P1a) or B/C-R (Pedotype 1b; P1b) profiles, respectively (Fig. 4B).

Pedotype	Macropedofeatures	Ichnofossils	Microfossil remains	Other features
P1a	Ferric rhizoliths, delicate rhizoliths, massive horizons, relict sedimentary structures	*Celliforma roselli, Celliforma argentina, Fictovichnus gobiensi, Feoichnus chall, Taenidium barretti*	Exclusive elements: cavate, puzzle and boat-type phytoliths, fragmented and whole sponge spicules, preserved epidermis. Non-exclusive: unicellular, multicellular and eroded phytoliths, charcoals, palynomorphs, radiolarians	Fossil bones
P1b	Ferric rhizoliths, delicate rhizoliths, mottles, incipient soil structure, massive or relict sedimentary structures	*Celliforma rosellii, Celliforma argentina, Palaeophycus tubularis, Planolites beverleyensis*	Exclusive elements: cavate, puzzle and boat-type phytoliths, fragmented and whole sponge spicules. Non-exclusive: unicellular, multicellular and eroded phytoliths, charcoals, palynomorphs, radiolarians	Fossil bones
P2	Calcareous rhizoconcretions, calcareous nodules, Fe-oxides rhizoliths, delicate rhizoliths, slickensides,	Mammal footprints, undifferentiate burrows	Exclusive elements: oblong and tower phytoliths. Non-exclusive: unicellular, multicellular and eroded phytoliths, charcoals, palynomorphs and radiolarians	Desiccation cracks, vertebrate fossil remains
P3	Fe-rich rhizoliths, delicate rhizoliths slickensides, mottles, angular/subangular blocky or wedge-shaped peds	*Celliforma rosellii, Celliforma argentina, Fictovichnus gobiensis*	Exclusive elements: cyperoid elongate, saddle, slightly bilobate, plurilobate and echinate globular phytoliths, stomatocys and diatoms. Non-exclusive: unicellular, multicellular and eroded phytoliths, charcoals, palynomorphs, radiolarians,	Fossil bones

Table 2. Main macropedofeatures, ichnofossils, microfossil remains, and other features of the paleosols of the Santa Cruz Formation.

Pedotype 1a: The incipient A/C horizon of the P1a (n=68; 60% of all paleosols in the measured sections) is non-structured and massive, with no ped development or with relict primary structures (Fig. 4B and C). The most conspicuous macropedofeature of the P1a paleosols are ferric and delicate rhizoliths (Fig. 4C; Table 2). Other types of bioturbation are due to the occurrence of undifferentiated burrows of the following types: *Celliforma rosellii, Celliforma argentina*, *Fictovichnus gobiensis*, *Feoichnus challa*, and *Taenidium barretti* (Table 2). Fossil bones and microfossil remains (Table 2) are found in this pedotype (see below). At the micro scale, the A/C horizon (Fig. 4D–E) shows fine to coarse sand particle size classes, and a coarse/fine (c/f) ratio (c/f = 3.1 μm) of 10/1 with a coarse monic distribution. The matrix grains are made up of fresh quartz, together with pumiceous fragments, plagioclases, k-feldspars, volcanic lithics (felsic and pilotaxic texture), and sedimentary grains, all of which have a low to moderate degree of alteration. Grains of biotite, amphiboles, and epidote are also present. The voids are characterized by simple packing, and scarce biogenic channels (Fig. 4E), and chambers. Scarce small pedogenic Fe-Mn nodules with amiboidal shape are the only pedofeature observed at this scale (Fig. 4D). The non-clay mineral species identified by XRD in the P1a are, in decreasing order of abundance, quartz and feldspars; small and very small amounts of opal, calcite, and/or clinoptilolite are also present in some samples. The clay mineralogy of this pedotype is dominated by smectite (100–40%), with minor proportions of illite (<40%), chlorite and illite/smectite mixed-layers (<20%), and kaolinite (<5) (Fig. 4F).

Pedotype 1b: This pedotype (n=12; 11% of all paleosols in the measured sections) is characterized by a B/C horizon (Fig. 4B). In contrast with the A/C horizons of P1a, which are defined by the occurrence of bioturbation and relict primary structures, B/C horizons are composed of beds that contain features of B horizons (rhizoliths, slickensides, fossil traces, incipient soil structure) and preserve characteristics of C horizons (some primary sedimentary

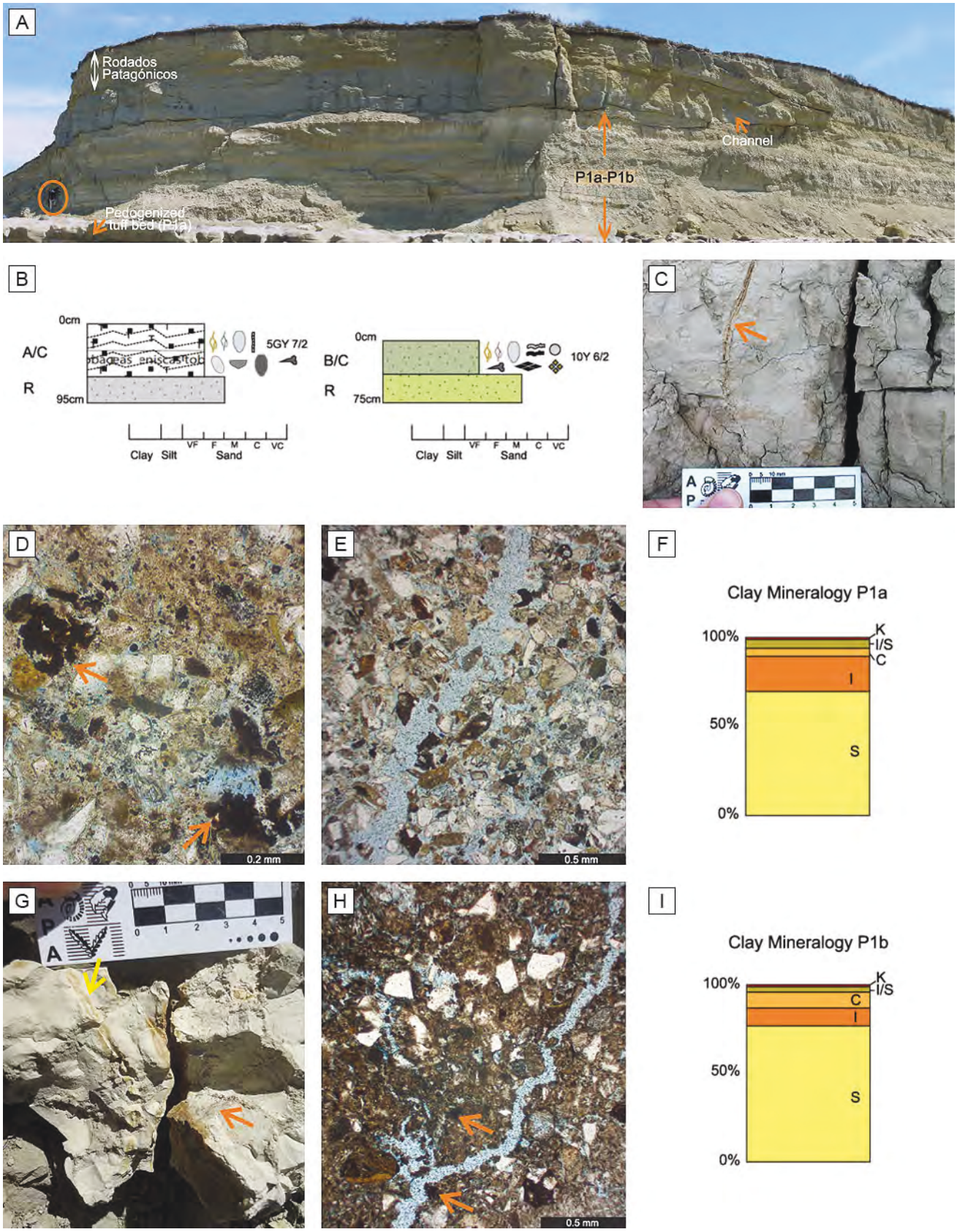

Figure 4. Pedotype 1 (P1a-P1b). **a)** Appearance of the stacked P1a and P1b paleosols at Cañadón Las Totoras locality. Note the person as scale in the left corner (circle). **b)** Representative profiles of P1a and P1b, respectively (see explanation of Figure 2 for macrofeatures). **c)** Detail of a ferric rhizolith in P1a (scale in centimeters). **d)** Microscopic view of strongly impregnated amiboidal shaped Fe-Mn nodules in P1a. Note that grains of the groundmass show low to middle degree of alteration (PN, 10x).

structures or massive) (Fig. 4B). At the macro scale, P1b is identified by ferric and delicate rhizoliths, mottles, and ichnofossils such as undifferentiated burrows, *Celliforma rosellii*, *Celliforma argentina*, *Palaeophycus tubularis*, and *Planolites beverleyensis* (Table 2). Fossil bones and microfossil remains (Table 2) are recognized at these levels (see below). This pedotype is micromorphologically characterized by very fine to fine sand particle size classes with a small amount of medium to coarse sand-sized particles (Fig. 4H). The c/f ratio (c/f = 3.1 μm) is 10/1 with a monic distribution, or it is 1/3 with an open porphyric distribution (coinciding with areas where the color of the groundmass is light to dark brown and probably obscured by organic matter), with a speckled and granostriated b-fabric. Components of the coarse fraction are moderately altered volcanic and sedimentary lithic fragments and pumiceous fragments, together with cuspate glass shards and grains of plagioclase with a low to moderate degree of alteration, and scarce fresh quartz grains. Intraclasts —derived from older paleosols (pedorelicts) or unmodified underlying strata— and phytoliths are distinguished at the micro scale. Opaque minerals as well as biotite and amphibole grains are also present. Massive to weak subangular blocky arrangement occurs in this horizon. The voids of this pedotype are simple packing voids, planar voids, vughs, and biogenic channels and chambers (Fig. 4H). Micropedofeatures are scarce small Fe-Mn oxide nodules with amiboidal shape (Fig. 4H). Non-clay minerals identified by XRD in the P1b consist in quartz and feldspars with low proportions of opal. Clay minerals include smectite (85–70%), with lesser amounts of illite (15–5%), chlorite (<10%), illite/smectite mixed- layers (<5%), and kaolinite (traces) (Fig. 4I).

Pedotype 2 (P2)

The P2 pedotype (n=17; 15% of all paleosols in the measured sections) is found in pinkish gray (5YR 8/1) to dusky yellow green (5GY 5/2) massive silty–clayey facies (Fm), and in a lesser proportion over massive tuffaceous facies (Sm and Tm, respectively) (Table 1; Figs. 2 and 5). It is an infrequent paleosol in the analyzed SCF succession, and it occurs mainly in the middle part of the unit (Fig. 2). P2 is defined as a grayish-greenish paleosol with calcareous rhizoconcretions, calcareous nodules, Fe-oxides rhizoliths, delicate rhizoliths, slickensides, desiccation cracks, mammal footprints, and other types of bioturbation such as undifferentiated burrows (Fig. 5A–D; Table 2). Vertebrate fossil and microfossil remains are sometimes present in this pedotype (see below and Table 2). Horizons of P2 are non-structured and massive, without ped development, and constitute profiles with A/C-R, A-Bk-C or Bk-C horizons (see Fig. 5B for features of each horizon).

At the micro scale (Fig. 5E–G), the coarse fraction of the Bk horizons is made up of fresh quartz, plagioclases with low degree of alteration together with cuspate glass shards, pumiceous fragments, volcanic lithics, and sedimentary fragments with variable (low–high) degree of alteration. Amphiboles, opaque minerals, and intraclasts derived from older paleosols or unmodified underlying strata also occur. The mineral coarse fraction is composed of coarse silt to medium sand grains. The c/f ratio (c/f = 3.1 μm) varied from 1/9 to 3/7, with an open porphyric distribution. The groundmass is light to dark brown, probably due to the presence of organic matter and/or micrite. The b-fabric is stipple-speckled to cross-striated, and/or crystallitic. Subangular blocky peds defined by planar voids show internally granular peds with shrinkage and circumgranular porosity (Fig. 5E), or there are massive arrangements. Compound packing voids, vughs, and planar voids are preserved in the groundmass. The pedofeatures are: microsparry to sparry coatings around wall voids and dense complete infillings of the same material (Fig. 5F); abundant Fe-Mn oxides and organic matter coatings, as well as scarce clay coatings around peds and planar voids; scarce massive carbonate nodules; abundant small Fe-Mn oxides nodules with amiboidal shape; and abundant very porous microaggregates of co-

e) Simple packing voids and a biogenic channel in P1a (PN, 4x). **f)** Average data of clay mineralogy (S: smectite; I: illite: C: chlorite; I/S: illite/smectite mixed-layers; K: kaolinite) in P1a. **g)** Fe-rich rhizoliths (yellow arrow) and slickensides (orange arrow) in P1b (scale in centimeters). **h)** Simple packing and planar voids that define incipient subangular microblocky peds at P1b. Note the dark brown color of the groundmass. Arrows indicate small Fe-Mn nodules (PN, 4x). **i)** Average data of clay mineralogy (S: smectite; I: illite: C: chlorite; I/S: illite/smectite mixed-layers; K: kaolinite) in P1b. PN: parallel nicols.

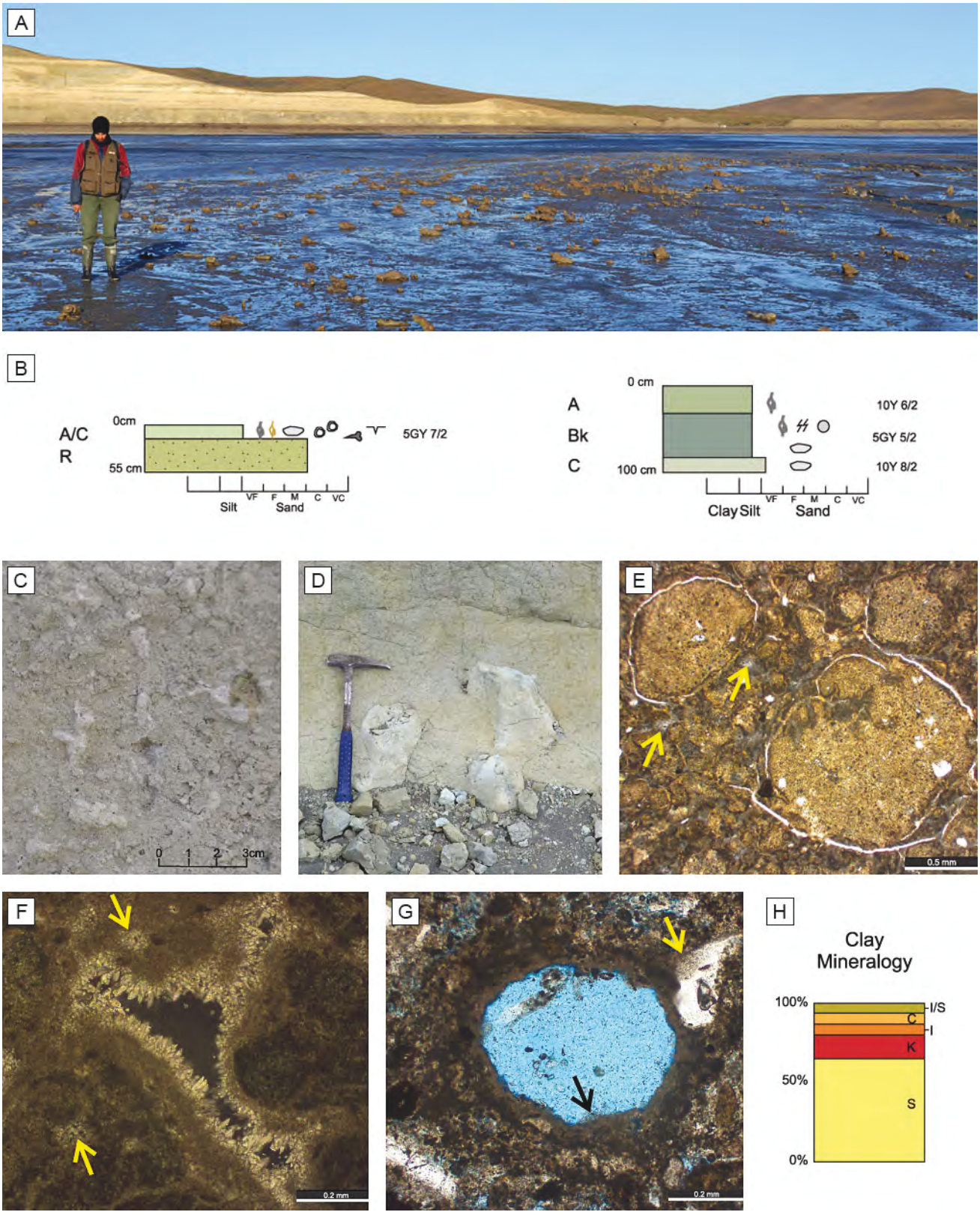

Figure 5. Pedofeatures of Pedotype 2 (P2). **a)** View of the calcareous nodules of the P2 outcropping in the current intertidal zone to the south of the Cañadón Las Totoras locality. **b)** Representative profiles of P2 (see explanation of Figure 2 for macrofeatures). **c)** Carbonatic rhizoconcretions in an A horizon. **d)** Carbonatic nodules in a Bk horizon (the pick is 33 cm-long). **e)** Internal granular peds with shrinkage and circumgranular porosity. The arrows indicate microsparite patches in the groundmass (PN, 4x). **f)** Sparitic coatings around a wall void. Note the dense, complete infillings of the same material (arrow) (XN, 10x). **g)** Rhizocretion around a root cavity (pedotubule). The yellow arrow shows a floating etched grain, and the black arrow marks a coating of fibre

alescent excrements. Rhizocretions (*sensu* Klappa, 1980) around root cavities (pedotubules), coatings of fibre calcite lying perpendicularity to the surface of these root cavities, floating and etched skeleton grains, and bladed calcite coronas are observed at a micro scale (Fig. 5G). Compositionally, the non-clay minerals identified by XRD are, in decreasing order of abundance, calcite, quartz, and feldspars, together with very small amounts of opal. The clay minerals of the P2 (Fig. 5H) are characterized by the dominance of smectite (90–40%), with a lesser amount of illite and illite/smectite mixed-layers (25–5%), kaolinite (<20%), and chlorite (<10%).

Pedotype 3 (P3)

The P3 pedotype (n=16; 14% of the all paleosol profiles in the measured sections) is found in the middle and in the bottom of the lowermost upper part of the SCF (Fig. 2) with low relative abundance. It is developed on pale olive (10Y 6/2) to 5Y 4/4 (moderate olive brown) massive tuffs (Tm facies), massive sandy facies (Sm), massive or laminated silty–clayey facies (Fm and Fl, respectively) (Table 1; Figs. 3 and 6). This pedotype is defined as an olive-colored paleosol with Fe-rich and delicate rhizoliths, *Celliforma rosellii*, *Celliforma argentina*, *Fictovichnus gobiensis,* slickensides, mottles, and angular/subangular blocky or wedge-shaped structure (Fig. 6B–D; Table 2). Fossil mammal and microfossil remains are present in this pedotype (see below and Table 2). This pedotype constitutes profiles with A-Bss1-Bss2-Bss3-C or R, A-Bss, or Bss-C or R horizons (see Fig. 6B for features of each horizon).

At a micro scale (Fig. 6E–H), the coarse fraction of the Bss horizons is made up of quartz, k-feldspars, and plagioclases with low degree of alteration, glass shards (planar and cuspated shape) and pumiceous fragments with medium to high degree of alteration (Fig. 6E). In addition, there are volcanic lithic fragments with pilotaxic and trachytic textures with fresh to low degree of alteration (Fig. 6E), and fragments of sedimentary rocks. Grains of amphibole, epidote, biotite, and opaque minerals, as well as phytolithic remains and diatoms also occur in the coarse fraction. The Bss horizon shows fine siltstone to medium sand particle size classes. The mineral coarse fraction is composed of medium sand grains. The c/f ratio (c/f = 3.1 μm) ranges from 3/1 to 1/9 with an open to closed porphyric distribution. The groundmass is light to dark brown, probably in part due to the presence of organic matter. The b-fabric is granostriated (Fig. 6F), reticulated, speckled, and undifferentiated. Blocky peds defined by channels and planar voids are common (Fig. 6G). Internal wedge-shaped micropeds, granular micropeds, and angular to subangular blocky micropeds are observed. Compound packing voids, chambers, channels, and vughs are preserved in the groundmass. The pedofeatures are clay coatings and Fe-Mn oxide coatings around wall chambers and channels; loose discontinuous infillings of dark or light groundmass inside chambers and vughs, and dense incomplete infillings of zeolites (clinoptilolite) inside vughs. Also there are coatings; hypocoatings, and quasicoatings of organic matter around planar and channel voids (Fig. 6G); scarce to abundant Fe-Mn oxides and Mn oxides aggregated nodules with amiboidal shape (Fig. 6H) or typic; abundant very porous microaggregates of excrements (Fig. 6H); and scarce pedorelicts or intraclasts.

Non clay minerals determined from XRD analyses are, in decreasing order of abundance, quartz and feldspars with small amounts of opal, clinoptilolite and calcite. Clay minerals consist mainly of smectite (95–80%) with a low proportion of illite (<10%), chlorite (<10%), and illite/smectite mixed-layers (<5%) (Fig. 6I).

MICROREMAINS DATASET OF THE SANTA CRUZ FORMATION

Although the majority of the analysed paleosols (75% of the total samples) preserves phytoliths and microfossil remains, a minor portion of the studied paleosols (25% of the total samples), mainly from P1 and P3, do not present microremains. Within the fertile samples, there are a 15% of samples that do not present sufficient abundance of remains to be considered in the statistical analyses. For this reason, we have been able to describe and compare in-group form only according to the pedotype to which they belong (Fig. 7A; Table 2).

calcite (PN, 10x). **h)** Average data of clay mineralogy (S: smectite; K: kaolinite; I: illite; C: chlorite; I/S: mixed layers of illite/smectite) in P2. PN: parallel nicols: XN: crossed nicols.

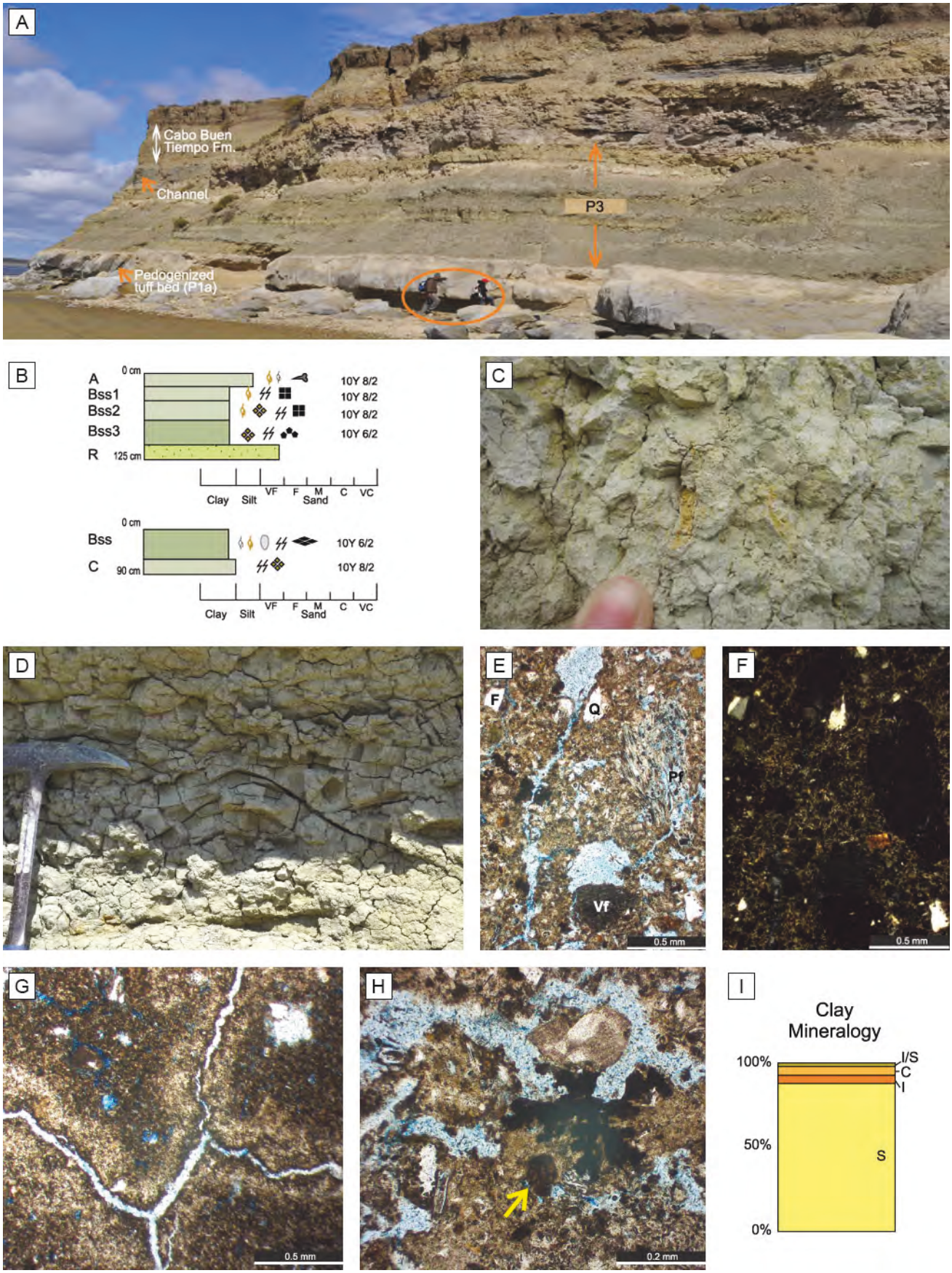

Figure 6. Pedotype 3. **a)** General aspect of stacked P3 paleosols overlain by a channeled-body at Killik-Aike Norte locality. Note people for scale (circle). **b)** Representative profiles of the P3 (see explanation of Figure 2 for macrofeatures). **c)** Fe-rhizoliths

From the comparative analysis of the presence and abundance of the main phytolith morphotypes (Fig. 7B), clear similarities can be observed between the compositions (Fig. 8) of the three pedotypes. This is especially apparent from the greater abundance of elongated elements (Fig. 8R), as well as polyhedral (Fig. 8Q), fan-shaped (Fig. 8P), point-shaped (Fig. 8E), and different globular (Fig. 8C and D) phytoliths. The exclusive presence of particular elements characterizes each pedotype (Table 2). Thus, cavate, puzzle (Fig. 8G), and boat-type (Fig. 8B) phytoliths belong to P1 (Fig. 7 and Table 2) demarcate the presence of dicots and microthermal grasses (C_3 plants). Oblong elements belong to P2 (Fig. 7 and Table 2); while, cyperoid elongate phytolths belong to P3 (Fig. 7 and Table 2). Tower elements are the dominant form in P2; meanwhile, saddle, slightly bilobate, plurilobate (Fig. 8B), and echinate globular (Fig. 8C) phytoliths are the most abundant elements in P3. This indicates a greater abundance of temperate elements in P2, whereas in P3 there are megathermal elements (C_4 plants) that suggest variable conditions in hydric availability. Multicellular phytoliths (mainly formed by fragments of woody tissue) and eroded phytoliths (Fig. 8M) are also present in the three pedotypes. Similarly, large elements (elongate, polyhedral, and fan-shaped types) with different degree of erosion were also observed. Non-phytolith microremains, such as charcoals (Fig. 8N), palynomorphs (Fig. 8K), and radiolarians (Fig. 8I) occur in all the pedotypes. Stomatocys (Fig. 8L) and diatoms (Fig. 8L) are exclusively present in P3 (Fig. 7 and Table 2). Fragmented and whole sponge spicules (Fig. 8O) characterize P1 (Fig. 7 and Table 2). Particularly, in one sample of the P1, preserved epidermis with siliceous elements has been found (Fig. 7, 8A and Table 2). It has a marked graminoid affinity, with a disposition of zoned epidermal elements (in costal and intercostal areas) with several rows of costal short cells, with elongated saddle-shaped siliceous elements. The intercostal zone has a band of two rows of stomata with low dome-shaped, ovoid, cells; the width of the subsidiary cells smaller in relation to the horizontal length, and the presence of hooks. Cells in the middle part of the intercostal zone are interrupted by single saddle square short cells. Although this set of characters does not allow the determination of its affinity at a specific level, it demonstrates a clear chloridoid affinity (C_4 plants).

VERTEBRATE-BEARING PALEOSOLS

Vertebrate fossils were recorded in levels of the P2, the middle part of the unit, in the area of Monte Tigre, very near to the Cañadón Las Totoras locality, and at Cañadón Palos (see Figs. 1B and 2). These fossils include mostly rodents, xenarthrans (sloths and cingulates), litopterns and notoungulates (both typotheres and toxodontians) (Table 3). In a preliminary taxonomic approach, taxa collected were similar to those recorded from the best-known northern localities such as Puesto La Costa and Estancia La Costa (Estancia La Costa Member) (*e.g.*, Vizcaíno *et al.*, 2012) (see Fig. 1B). To date, no taxa found in the upper member are absent in the lower member, although the proportions of different mammalian taxa appear to be different.

DISCUSSION

Pedogenesis

Paleosols classification: Very poorly defined soil horizons of the P1a, with scarce macrofeatures (bioturbation), preservation of sedimentary structures, and a low to medium degree of alteration of the coarse components suggest very weak pedogenic modification (*e.g.*, Retallack, 2001). These features are similar to modern Entisols (*i.e.*, immature soils with a very poor degree of development that can have little or no development of pedogenic horizons, following Soil Survey Staff, 1999; Buol *et al.*, 2011; Schoeneberger *et al.*, 2012). Thus, P1a is classified and interpreted as a paleo-Entisol (Retallack, 2001), and as a Protosol

and subangular blocky peds in a Bss horizon. **d)** Conjugate slickensides that define wedge-shaped peds in a Bss horizon. **e)** Microscopic view of the light to dark brown groundmass and the coarse fraction of the P3 showing medium sand particles of volcanic (Vf) and pumiceous (Pf) fragments, quartz (Q) and feldspar (F) (PN, 4x). **f)** Same field as in e showing a granostriated b-fabric (XN, 4x). **g)** Planar and channel voids that defined strongly developed blocky peds (PN, 4x). **h)** Detail of strongly impregnated amiboidal Fe-Mn nodule. The arrow marks an oval microaggregated (excrement) (PN, 10x). **i)** Average data of clay mineralogy (S: smectite; I: illite; C: chlorite; I/S: mixed layers of illite/smectite) in P3. PN: parallel nicols; XN: crossed nicols.

MONTE TIGRE LOCALITY (CLOSE TO CAÑADÓN LAS TOTORAS LOCALITY)

Marsupialia
- Sparassodonta indet.

Litopterna
- Proterotheriidaeindet.

Notoungulata
- Typotheria
  - Interatheriidae
    - *Protypotherium* sp.
  - Hegetotheriidae
    - cf. *Interatherium*
- Toxodontia
  - *Adinotherium* sp.
  - *Nesodon* sp.

Astrapotheria
- cf. *Astrapotherium*

Xenarthra
- Cingulata
  - Glyptodontidae
    - Propalaeohoplophorinaeindet.
    - *Eucinepeltussp.*
  - Dasypodidae
    - *Prozaedyussp.*
- Folivora
  - Eucholoeopsingens
  - *Eucholoeops* sp.
  - *Pelecyodon* sp.
  - *Nematherium* sp.

Rodentia
- Erethizontidae
  - *Steiromysduplicatus*
- Chinchilloidea
  - *Prolagostomus* sp.
- Cavioidea
  - *Eocardia* sp.
  - *Neoreomys* sp.

Aves
- Cariamidae indet.

CAÑADÓN PALOS LOCALITY

Marsupiala
- Abderitidae
  - cf. *Abderites*

Litopterna
- Proterotheriidaeindet.

Notoungulata
- Toxodontia
  - *Adinotherium* sp.

Rodentia
- Cavioidea
  - *Neoreomys* sp.
- Chinchilloidea
  - *Perimys* sp.

Table 3. Preliminary faunal list of the Santa Cruz Formation at the studied localities.

(Mack *et al.*, 1993). P1b is similar, but slightly more developed paleosols. This is based on poorly defined soil horizons (B/C profiles), a low to medium degree of alteration of the coarse components, poorly developed peds at the micro scale, and the scarcity of micropedofeatures (*i.e.*, nodules). These features are evidence of limited pedogenesis (*e.g.*, Retallack, 2001). Modern Inceptisols are immature soils with weak development that lack many diagnostic features, but they are characterized by poor- to moderate-development of soil horizons (*e.g.*, Soil Survey Staff, 1999; Buol *et al.*, 2011; Schoeneberger *et al.*, 2012). Although the occurrence of slickensides and incipient blocky or wedge-shape peds such as those of P1b are features of a more mature soil order such as Vertisols (*e.g.*, Retallack, 2001), these features in P1b paleosols are incipient and this pedotype lacks other diagnostic feature of Vertisols. Consequently, P1b may be classified and interpreted as a paleo-Inceptisol (Retallack, 2001) and as a vertic Protosol (Mack *et al.*, 1993) (*i.e.*, Inceptisol with vertic features).

The P2 paleosol type displays poor- to moderately-defined horizons (A/C-R, A-Bk-C, Bk-C) with non-structured B horizons, poorly preserved primary sedimentary structures, and weakly to moderately altered coarse components. These features are evidence of limited pedogenic modification and are consistent with modern Inceptisols (Soil Survey Staff, 1999, Retallack, 2001; Schoeneberger *et al.*, 2012). Due to the presence of a calcic horizon, P2 is classified and interpreted as a paleo-calcic Inceptisol, and as a Calcisol (Mack *et al.*, 1993; Retallack, 2001).

The P3 paleosol type shows moderate- to well-developed horizons (profiles A-Bss1-Bss2-Bss3-C, A-Bss, or Bss-C). Given the abundance of pedogenic slickensides and the occurrence of blocky aggregates at a macro scale, abundant fine and very-fine particle size classes (clay), and the dominance of smectite in the clay fraction, P3 is classified and interpreted as a paleo-Vertisol (Soil Survey Staff, 1999; Retallack, 2001; Schoeneberger *et al.*, 2012), and as a Vertisol (Mack *et al.*, 1993).

Pedogenic processes and paleosol development: Macro and micromorphological features, and mineralogical data of the paleosols of the SCF indicate that the main pedogenic processes were, in decreasing order of magnitude, bioturbation, vertization, calcification, gleization, illuviation, and melanization (see Table 4). Alluviation (*sensu* Fanning and Fanning,

1989) was a subordinated process (Table 4).

Macro- and micropedofeatures are useful indicators of paleosol development (*e.g.*, Birkeland, 1999; Retallack, 2001) because the time that they take to form varies considerably. The P1a and P1b paleosols (Entisol- and Inceptisol-like paleosols; Protosols) are very weakly and weakly developed paleosols, respectively. Pedofeatures of Entisol-like paleosols might develop in a rather very short time span (10^1–10^2 yr). By contrast, morphological features of paleo-Inceptisols take a few thousand years to develop (10^2–10^3 yr) (*e.g.*, Birkeland, 1999; Retallack *et al.*, 2000; Retallack, 2001). The occurrence of calcic nodules and rhizoconcretions within the calcareous horizon (Bk) of Pedotype 2 are characteristics of Stages II and II–III, respectively, of Gile *et al.* (1966) and Machette (1985), and thus, they represent weakly developed calcretes or calcic paleosols (*e.g.*, Alonso-Zarza *et al.*, 1998; Sacristán Horcajada *et al.*, 2016). Calcretes of the P2 paleosol type are similar to those of the lower part of the SCF at the Puesto La Costa locality (north of the study area), recently described by Raigemborn *et al.* (2018a). This calcrete type refers to short pedogenesis and involves a few several hundred to a few thousand years of soil formation (*e.g.*, Retallack *et al.*, 2000; Retallack, 2001). Modern vertisols are soils that can form in a short time (10^1–10^2 years; Birkeland, 1999; Retallack, 2001; Buol *et al.*, 2011). However, the Vertisols (P3) of the SCF are interpreted as weakly to mildly developed paleosols due to the occurrence of blocky aggregates at the macro- and microscale, and clay coatings, which suggests formation over more than 10^3 years but less than 10^4–10^5 years due to the absence of an argillic (Bt) horizon (*e.g.*, Birkeland, 1999; Retallack, 2001).

The vertical arrangement of paleosols within the analyzed section of the SCF is quite characteristic. It starts with weakly developed paleosols (mainly P2) in the middle part of the unit, more developed soils (P3) in the bottom of the lowermost upper part of the SCF, and very weakly- and weakly-developed ones (P1a and P1b) in the upper part of the succession (see Fig. 3). Thus, a slight stratigraphic regression in the degree of development of the paleosols of the SCF can be inferred (see below).

Terrestrial landscapes of the Santa Cruz Formation

The combination of abiotic (*i.e.*, paleosols) and biotic data (*i.e.*, soil fauna and flora, as well as vertebrate fauna) of the middle–upper SCF beds permits reconstruction of landscapes and soil ecosystems, and allows us to describe their evolution during the early Miocene. This is because paleosols can be used to estimate, for example, the effects of rates of sedimentation, erosion, time of exposure, climate, and hydrologic conditions on terrestrial landscapes and soil ecosystems evolution (*e.g.*, Kraus, 1999; Retallack, 2001; Hasiotis *et al.*, 2007; Catena *et al.*, 2016; Hembree and Bowen, 2017; Raigemborn *et al.*, 2018b).

Sedimentation rate and time of exposure: The analyzed successions of the SCF correspond to stacked paleosols (with variable degrees of development) formed mainly on fluvial floodplains that are interbedded with non-pedogenically modified beds. This situation indicates that periods of geomorphological instability (*i.e.*, sedimentation and erosion) were punctuated by pauses in deposition or by a decreased sediment accumulation rate (*i.e.*, intervals of landscape stability and pedogenesis). Consequently, the type of paleosol that formed depended on how rapidly the sediments accumulated, whether the sedimentation was continuous or discontinuous; it also depended on the length of the pauses in accumulation (Kraus, 1999).

Considering the pedofeatures of the SCF's paleosols, we can establish that pauses in sedimentation/erosion during the studied time span (~ 1 My) were relatively short-term. These pauses varied from very brief (P1a; 10^1–10^2 yr) through short-lived (P1b, P2; 10^2–10^3 yr) to moderate (P3; ~10^3 yr).

Pedotypes P1a, P1b, P2, and some cases of P3, appear as compound soils with simple and stacked profiles. This results from rapid and episodic sedimentation (*e.g.*, Kraus, 1999), and suggests a high sedimentation/pedogenesis ratio. By contrast, multiple overlapping profiles of the P3 paleosol type (*i.e.*, multiple Bss horizons) suggest composite paleosols, which probably formed under slow, steady sedimentation (*e.g.*, Kraus, 1999), with a lower sedimentation/pedogenesis ratio than compound soils. Truncated-top profiles (*i.e.*, profiles without A horizon) in the P1b paleosol type and some cases of P2 and P3; together with the occurrence of pedorelicts and/or intraclasts in the groundmass, are evidence of erosion.

Paleoclimate: Because climate is a controlling factor on pedogenesis and on its degree of development

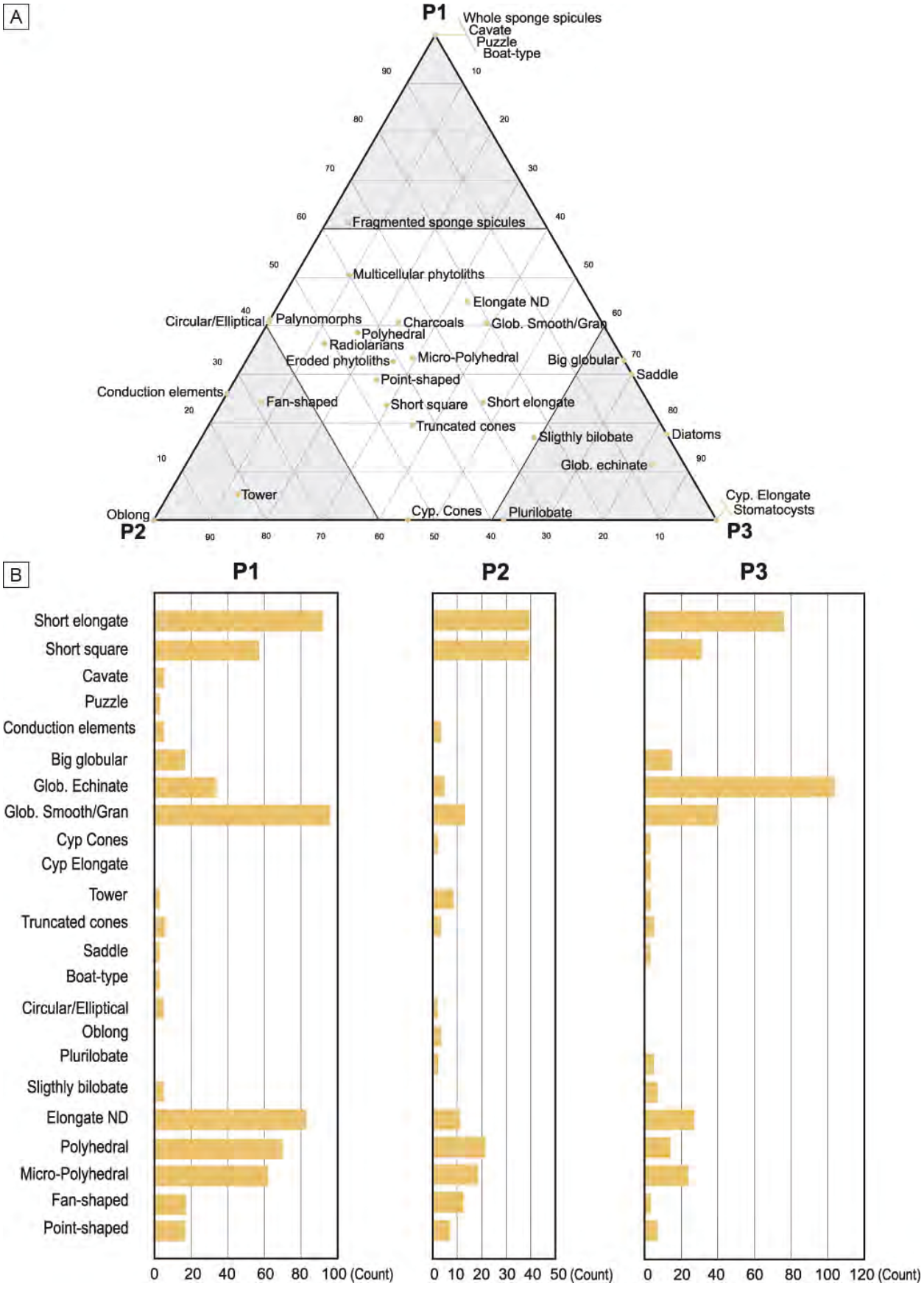

Figure 7. Abundance of phytoliths and microremains in the SCF's pedotypes. **a)** Ternary plot of abundances of the major types of phytoliths and microremains. **b)** Counting of the major types of phytoliths in each pedotype.

(*e.g.*, Retallack, 2001; Cecil and Dulong, 2003), paleosols can be used as a paleoclimate proxy. Modern Entisols and Inceptisols can be formed in different climates (Retallack, 2001). The low degree of development of these soils restricts paleoclimatic interpretations. However, the features of the P1a and P1b paleosol types (*e.g.*, minerals with low–moderate degree of weathering in the groundmass, poorly preserved primary structures, and smectite as the dominant clay-mineral) attest to relatively warm and humid conditions (Retallack, 2001), with seasonality in water availability (*e.g.*, Raigemborn *et al.*, 2018b). Seasonal rainfalls are also supported by the presence of slickensides, mottles, and striated b-fabric in the P1b paleosol type.

Pedogenic calcretes can form in climates with a wide range of rainfall (50–1000 mm yr^{-1}) and temperatures (very hot to cold) (Alonso-Zarza and Wright, 2010; Zamanian *et al.*, 2016) where the limit to calcite formation is the episodic drying of the soil for a long period (*e.g.*, Kraus and Hasiotis, 2006). Features and mineral composition of the P2 paleosol of the SCF (*e.g.*, dessication cracks, slickensides, weatherable minerals with variable degrees of alteration, striated b-fabrics, calcite, and abundance of smectite) attest to relatively warm and humid (~1000–1200 mm yr^{-1}) climates with seasonal rainfall (*e.g.*, Raigemborn *et al.*, 2018a).

Typically, modern Vertisols form when mean annual precipitation ranges from 800 to 1500 mm yr^{-1} with a pronounced dry season (Retallack, 2001; Sheldon and Tabbor, 2009). The occurrence of slickensides, mottles, striated b-fabrics, and an abundance of smectite (as occur in P3), suggests seasonal precipitation (*e.g.*, Raigemborn *et al.*, 2018b). These characteristics point to similar conditions to those inferred for the P1a and P1b paleosol types (*e.g.*, Hembree and Bowen, 2017), but probably in general terms slightly warmer and more humid as evidenced by the higher degree of alteration of the weatherable minerals in the groundmass of the paleosols.

Local hydrology and ecosystem: Dominance in smectite-content in all the pedotypes of the SCF attest to intermittently poorly drained conditions (Sheldon and Tabor, 2009). The pervasive reduced hues (gray–greenish or gray–olive) in the matrix of these paleosols suggest iron-depletion, implying that Fe was reduced and removed from these beds (PiPujol and Burrman, 1994; Kraus and Hasiotis, 2006). However, yellow-brown colors in ferric rhizoliths indicate the presence of goethite, and represent better-oxidized areas where the Fe was reprecipitated. The preservation of bone remains in all the analyzed pedotypes point to alkaline conditions and well-drained soils (Retallack, 2001; Bellosi and González, 2010).

Fe-Mn micro-nodules (evidence of redox cycles) and traces such as *Celliforma* (evidence of dry soils) and *Taenidium* (evidence of moderately- to well-drained soils) in P1a suggest that soil moisture regimes and drainage conditions fluctuated (*e.g.*, Retallack, 2001; Kraus and Hasiotis, 2006; Catena *et al.*, 2016, 2017; Hembree and Bowen, 2017). Consequently, P1a is indicative of moderately well-drained soils.

In the P1b paleosol type there is scarce evidence of redox cycles (*i.e.*, Fe-Mn micro-nodules). However, yellow-brown mottles, slickensides, and traces of *Celliforma* and *Planolites* attest to well-drained soils (Kraus and Hasiotis, 2006; Catena *et al.*, 2017; Hembree and Bowen, 2017). The presence of *Palaeophycus* indicates moderately to poorly-drained soils (Hembree and Bowen, 2017); meanwhile, the organic matter in the groundmass could be accumulated under wet conditions (Buol *et al.*, 2011).

P1 records a moderate diversity and moderate abundance of trace fossils dominated by Calichnia structures (*C. rosellii and C. argentina*). It also records Pupichnia structures such as *Fictovichnus*, nymph feeding chambers such as *Feoichnus*, meniscate trace fossils (*Taenidium*), simple sub-horizontal burrows (*Palaeophycus* and *Planolites*), and root structures. The P1 SCF trace fossil assemblage resembles the *Celliforma* Ichnofacies proposed by Genise *et al.* (2010). This ichnofacies was proposed for insect-dominated trace fossils assemblages developed in carbonate-rich paleosols in terrestrial or palustrine settings. In terrestrial settings, this ichnofacies indicates low plant coverage due to arid climate typical of desert shrubs and dry woodlands. In palustrine environments, it reflects the presence of bare soils preferred by wasps and bees for nesting after periodic water logging under sub humid to sub-arid climates. The SCF assemblage would represent an intermediate condition because it is neither marked by carbonate-rich paleosols nor by palustrine settings. The climatic conditions inferred based on the *Celliforma* ichnofacies is ambiguous due to it being preserved in sub humid to arid climates. However, at least temporary well drained soils with

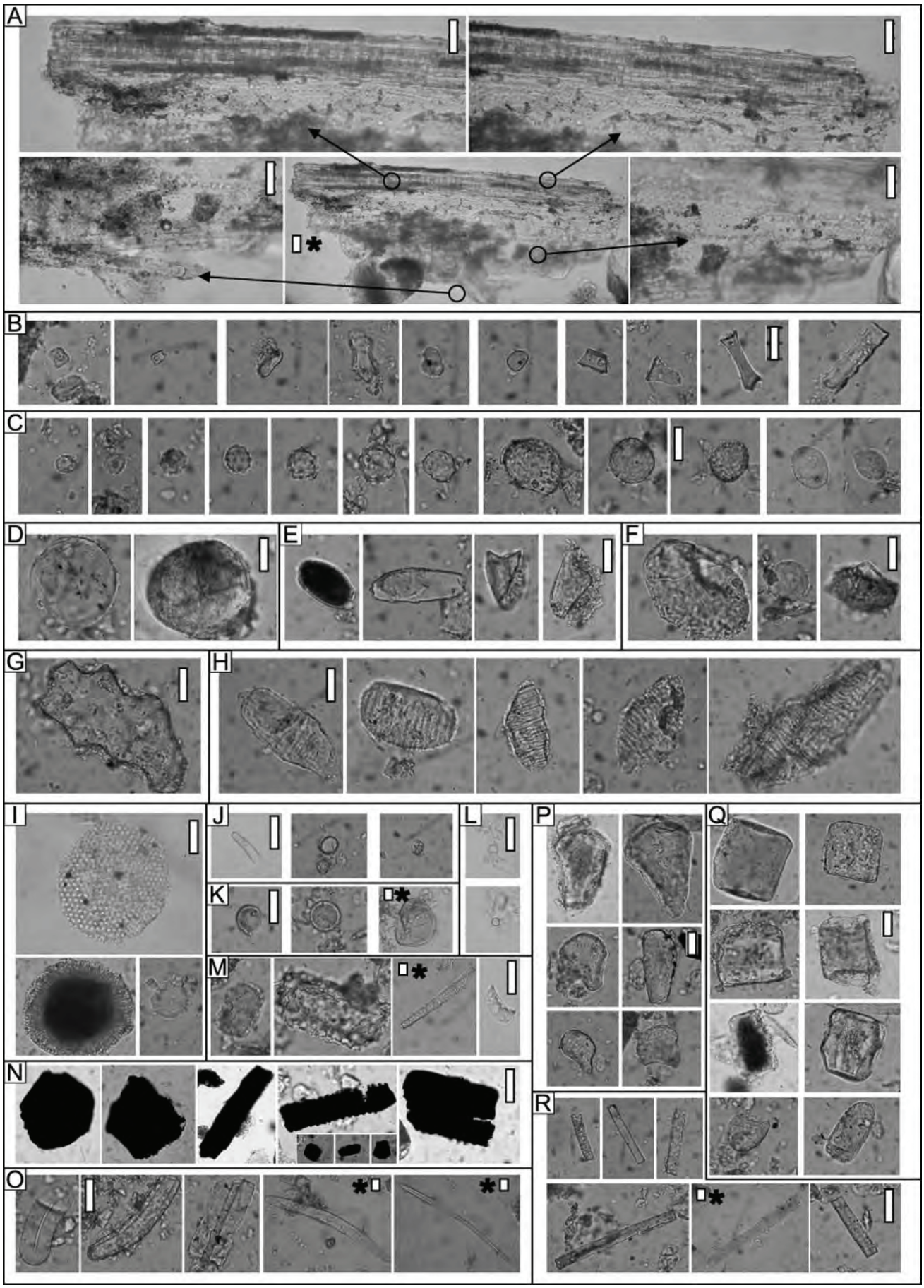
A
B
C
D
E
F
G
H
I
J
K
L
M
N
O
P
Q
R

relatively scarce vegetation cover are requirements for the establishment of wasp and bee nests (Genise *et al.*, 2010). Therefore, the P1b paleosol type is interpreted as a moderately-drained paleosol. Delicate rhizoliths in P1a and the mm-scale of the delicate and ferric rhizoliths of P1b denote colonization of the substrate by small-sized plants such as herbaceous dicots in the early stages of paleosol formation (Retallack, 2001; Catena *et al.*, 2016), which are typical of relatively open vegetated grassland-like soils (Retallack, 2001). Chambers of *Celliforma* in P1a and P1b also indicate environment with primary productivity, with reduced herbaceous vegetation cover (*e.g.*, Genise and Bown, 1994; Bellosi and González, 2010). In the same sense, the coexistence of dicot phytoliths (cavate and puzzle types) and festucoid elements in P1a and P1b, suggests the presence of a pasture with microthermal (C_3) components. The greater abundance of whole spicules in P1 attests to the existence of nearby watercourses.

Carbonatic pedofeatures, desiccation and shrinkage cracks, slickensides, Fe-rhizoliths and mottles, mammal footprints, and vertebrate fossil bones in P2 indicate well-drained soils and represent soils that undergo periodic drying (Retallack, 2001; Kraus and Hasiotis, 2006; Sheldon and Tabor, 2009; Zapata *et al.*, 2016; Raigemborn *et al.*, 2018a). However, the combination of these features with redox ones (gley matrix colors, Fe-Mn micro-nodules and coatings) together with scarce signs of improved soil drainage (coatings), are evidence of fluctuating soil moisture. Moreover, the mammalian footprints were produced in soupy to soft substrates, produced during periods of high-energy discharge of the fluvial system; these were later exposed, dewatered, and desiccated. Consequently, P2 is interpreted as a well-drained paleosol. The mm- and cm-scale of the rhizoliths and rhizoconcretions of P2 represent the roots of small- to medium-sized plants, which could characterize a relatively open wooded grassland-like soil (Retallack, 2001). Granular microstructure, as it appears in P2, is typically seen in grassland soils (Stoops *et al.*, 2010). Congruently, the major abundance of oblong, circular/elliptical and tower phytoliths together with silicified conduction elements, indicates an herbaceous community of low meadow with solitary arboreal elements or trees in small groups. Recorded vertebrate fauna at this pedotype shows a mixing of taxa adapted to open environments and to closed ones, as found in the lower fossiliferous levels of the SCF (*e.g.*, Puesto La Costa and Estancia La Costa; Fig. 1B) (see Vizcaíno *et al.*, 2010, 2012). Among taxa adapted to open environments are toxodontids such as *Adinotherium* (open habitats) and *Nesodon* (mixed habitats) (see Cassini, 2013). By contrast, climbing, arboreal sloths as *Eucholoeops* and *Pelecyodon* (Bargo *et al.*, 2012; Toledo, 2016), plus the tree-porcupine *Steiromys* (Candela and Picasso, 2008; Candela *et al.*, 2012), are indicative of vegetated areas covered by trees. Large sized mylodontoid sloths as *Nematherium* might have been more terrestrial, venturing out into open areas (Toledo, 2016). Some other taxa such as astrapotheres, proterotheriid litopterns, and propalaehoplophorine glyptodonts were also well-suited to living in closed, vegetated habitats (see Vizcaíno *et al.*, 2012; Cassini, 2013).

Similarly, to the other paleosols of the SCF, P3 shows evidence of a fluctuating water table. This is based on the occurrence of gley colors, Fe-Mn coatings and micro-nodules (signs of redox cycles), slickensides, *Celliforma*, and ferric-rhizoliths and mottles (evidences of well-drained conditions), together with the occurrence of diatoms in the groundmass. The latter is an indicator of soil moisture (Harris *et al.*, 2017). Also, there are signs of illuviation (coatings), which attest to improved soil drainage (Ashley and Driese, 2000). The P3 trace fossil assemblage is poorly diverse and moderately abundant. It is dominated by Calichnia structures (*C. rosellii and C. argentina*). It also records Pupichnia structures (such as *Fictovichnus*) and rhizoliths. The assemblage suggests temporary well-drained soils with relatively scarce vegetation cover as wasps and bees require

Figure 8. Microphotographs of microremains. **a)** Epidermal remains of a chloridoid grass with detailed views. **b)** Short cell phytoliths from grass (square, slightly bilobate, saddle-shaped, tower/truncated cones, and boat-type phytoliths). **c)** Globular elements. **d)** Big globular phytoliths. **e)** Point-shaped phytoliths. **f)** Cyperoid cones. **g)** Puzzle-type element. **h)** Conduction tissue elements. **i)** Radiolarian remains. **j)** Diatom fragments. **k)** Palynomorphs. **l)** Stomatocysts. **m)** Eroded phytoliths. **n)** Charcoals. **o)** Sponge spicules. **p)** Fan-shaped phytoliths. **q)** Polyhedral elements. **r)** Elongate phytoliths. Scale bar are 20 μm in all groups; * next to scale are out of scale.

for the establishment of nests (Genise *et al.*, 2010). Consequently, P3 is interpreted as a moderately well-drained soil that retains moisture in a seasonally dry environment with wet periods (*e.g.*, Kraus and Hasiotis, 2006). Small and short delicate rhizoliths in the P3 indicate that the vegetation was shallowly rooted, probably due to a relatively high water table, and consisted of small plants such as herbaceous dicots (*e.g.*, Retallack, 2001; Hembree and Bowen, 2017). Grasses and forbs dominate the vegetative cover on modern Vertisols (Buol *et al.*, 2011). Micro-granular peds and traces of *Celliforma* in the Vertisols of the SCF also indicate biological activity typical of grassland soils (Retallack, 2001; Bellosi and González, 2010; Stoops *et al.*, 2010). The predominance of chloridoid elements in P3, together with echinate globular phytoliths suggests megathermic (C_4) herbaceous vegetation with grasses and palms. Probably this ecosystem had been developed under conditions of dryness.

Paleolandscape reconstruction: Paleosols, ichnofossils, phytoliths, and fossil vertebrates of the middle and upper parts of the SCF at the southernmost extent of Santa Cruz province record past environmental, ecological, and climatic conditions that allow us to reconstruct southeast Patagonian landscape evolution during the early Miocene. Consequently, on the basis of the spatial distribution of the pedotypes of the SCF throughout the analyzed sections (see Fig. 2), three general terrestrial landscape stages (S1, S2, and S3) were defined (Fig. 9).

The landscape of the Stage 1 (S1) is represented by predominantly distal floodplain areas drained by confined and laterally stable channels (following Zapata, 2018) where mainly simple and stacked compound Calcisols formed (Fig. 9). Relatively limited pedogenic modification in P2 attests to intervals of rapid sedimentation during the middle part of the SCF. Calcisols were formed during short time spans (10^2–10^3 yr) of insignificant or null sedimentation rate and represent a relatively high sedimentation/pedogenesis ratio under relatively warm and seasonally humid conditions (Fig. 9). These conditions probably controlled the development of relatively dense vegetation integrated by trees, shrubs, palms, and low grasses (Fig. 9), and a scarce soil fauna. Well-drained soil conditions with fluctuating soil moisture also controlled the main pedogenic process (calcification) in the development of P2. Non-truncated profiles of this pedotype are indicative of relatively continuous aggrading environments; by contrast, truncated profiles attest to an unstable environment with repeated periods of erosion. On this landscape, the coexistence of vertebrate fauna adapted to open and closed habitats indicates a mixed environment involving open areas, alternating with patches of trees (Fig. 9). This interpretation is in agreement with the rest of the evidence analyzed here and with previous hypotheses by Vizcaíno *et al.* (2010). Namely, there is no clear evidence of the predominance of taxa adapted to open environments. Therefore, in contrast with the suggestion by Tauber (1997b), there is no evidence for a clear change from humid to arid habitats. In this regard, and conversely to the proposal by Tauber *et al.* (2004) of including Killik-Aike Norte within the Estancia La Costa Member (lower and middle parts of the SCF following Zapata, 2018), evidence analyzed here suggest that deposits at this locality would correspond to later stages of the SCF (Estancia La Angelina Member). In this sense, the occurrence of primates (see Tejedor *et al.*, 2006) in both lower and upper levels of the Killik-Aike Norte locality could be interpreted as an additional indicator of unchanging environments. Indeed, the primates recovered from the upper member of the SCF are not clearly distinguishable at the specific level from those recovered from the lower member. Currently these are all allocated to a single species, *Homunculus patagonicus* (Perry *et al.*, 2014). All living platyrrhines are arboreal and nearly all fossil platyrrhines (including all of the Patagonian ones) are reconstructed as arboreal. Therefore, the presence of primates in the vertebrate sample constitutes a reliable indicator of trees, at least at the depositional source.

The landscape of the Stage 2 (S2) corresponds to the bottom of the lowermost upper part of the SCF (lower Estancia La Angelina Member) where P3 are abundant (Fig. 9). Paleosols of the type P1 are also frequent. Following Zapata (2018), this stratigraphic interval of the SCF represents epiclastic distal floodplain settings and minor epi-pyroclastic proximal areas associated with simple and laterally stable as well as more sinuous channels. Floodplain zones in which P3 dominates were moderately modified by pedogenesis (Fig. 9). During this interval, periods of relatively slow and steady sedimentation with low sedimentation/pedogenesis ratio took place. Moderately-long (10^3 yr) pauses in accumulation

Pedotype	Macro, micro-features and clay mineralogy	Pedogenic processes
P1a	Macro: Rhizoliths, burrows, Celliforma rosellii, *Celliforma argentina, Fictovichnus gobiensis, Feoichnus challa, Taenidium barretti*	Bioturbation
	Micro: Channels and chambers	
P1b	Macro: Rhizoliths, burrows, *Celliforma rosellii, Celliforma argentina, Palaeophycus tubularis, Planolites beverleyensis*	
	Micro: Channels and chambers	
P2	Macro: Rhizoliths, mammal footprints, burrows	
	Micro: Excrements and granular peds	
P3	Macro: Rhizoliths, *Celliforma rosellii, Celliforma argentina, Fictovichnus gobiensis*	
	Micro: Chambers, channel, infillings of groundmass and excremen s	
P1a	Dominance of smectite	Vertization
	Macro: Blocky, wedge-shaped peds and slickensides	
P1b	Micro: Striated b-fabric and blocky peds	
	Dominance of smectite	
	Macro: Slickensides	
P2	Micro: Striated b-fabric, blocky peds, planar voids, shrinkage and circumgranular porosity	
	Dominance of smectite	
	Macro: Slickensides and blocky structure	
P3	Micro: Striated b-fabric, planar voids, blocky and wedge-shaped peds	
	Dominance of smectite	
P2	Macro: Calcareous rhizoconcretios and nodules	Calcificatio
	Micro: Crystallitic b-fabric, carbonatic coatings, infillings, odules, and bladed calcite coronas	
	Rhizocretions, pedotubles, coating of fiber calcite and floatin etched grains	
P1a	Macro: Fe-Mn nodules	Gleization
	Micro: Fe-Mn nodules	
P2	Macro: Fe-rich mottles and rhizoliths	
	Micro: Fe-Mn coatings and nodules	
P3	Macro: Fe-rich mottles and rhizoliths	
	Micro: Fe-Mn coating and Fe-Mn and Mn nodules	
P2	Micro: Clay, carbonatic, Fe-Mn and organic matter coatings	Illuviation
P3	Micro: Clay, Fe-Mn and organic matter coatings, organic matter hypocoatings and quasicoatings	
P1b	Light to dark brown color of the groundmass	Melanization
P2	Light to dark brown color of the groudmass and organic matter coatings	
P3	Light to dark brown color of the groundmass and organic matter hypocoatings, quasicoatings and coatings	
P1b, P3	Pedorelicts	Alluviation

Table 4. Pedogenic processes of the Santa Cruz Formation based on macro and microfeatures and clay-mineral data.

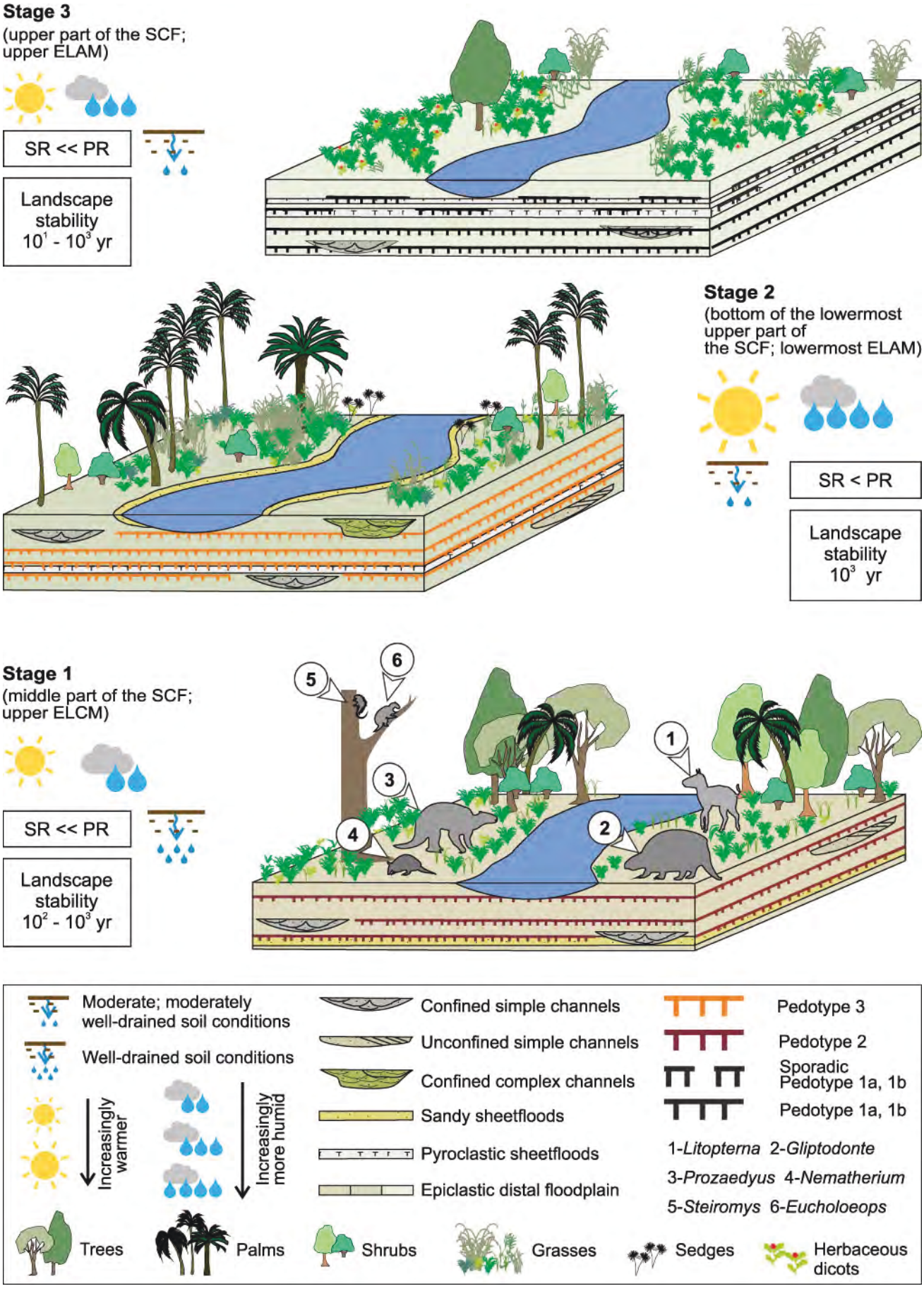
Stage 3
(upper part of the SCF; upper ELAM)
SR << PR
Landscape stability
10^1 - 10^3 yr
Stage 2
(bottom of the lowermost upper part of the SCF; lowermost ELAM)
SR < PR
Landscape stability
10^3 yr
Stage 1
(middle part of the SCF; upper ELCM)
SR << PR
Landscape stability
10^2 - 10^3 yr
1
2
3
4
5
6
Moderate; moderately well-drained soil conditions
Well-drained soil conditions
Increasingly warmer
Increasingly more humid
Trees
Palms
Confined simple channels
Unconfined simple channels
Confined complex channels
Sandy sheetfloods
Pyroclastic sheetfloods
Epiclastic distal floodplain
Shrubs
Grasses
Pedotype 3
Pedotype 2
Sporadic Pedotype 1a, 1b
Pedotype 1a, 1b
1-Litopterna 2-Gliptodonte
3-Prozaedyus 4-Nematherium
5-Steiromys 6-Eucholoeops
Sedges
Herbaceous dicots

gave way to the formation of composite paleo-Vertisols, which developed over distal floodplain areas under seasonal and slightly warmer and more humid conditions than those interpreted for the formation of P1a and P1b of the following Stage 3 (Fig. 9). This climatic interpretation, together with moderately well-drained soil conditions and a seasonal relatively high water table conditioned the vertization that was the main pedogenic process in P3. A soil biota that mainly included grasses and palms adapted to variable conditions in hydric availability (C_4 plants) (Fig. 9), solitary bee larvae, and adult and nymph soil beetles characterized these longer intervals of landscape stability.

Towards the upper part of the SCF (upper Estancia La Angelina Member), epiclastic and pyroclastic distal and proximal floodplains drained by simple and laterally stable channels (Zapata, 2018), mainly associated with Protosols (P1a and P1b) characterized the landscape of the Stage 3 (S3) (Fig. 9). Here, periods of rapid and episodic deposition prevailed, punctuated by very short–short periods of pedogenesis (10^1–10^3 yr) with high ratios of sedimentation/pedogenesis which gave way to compound paleo-Entisols and -Inceptisols (P1a and P1b). These pedotypes formed under similar climatic conditions to those inferred for the S1 stage, but slightly more humid or less seasonal that in S1 based on the lack of calcareous features. Truncated profiles and pedorelicts in P1b represent formation on an unstable landscape (*i.e.*, erosional events). In this context, in temporally stable environments with moderately well-drained (P1a) and moderately-drained (P1b) soil conditions developed a microthermic (C_3) herbaceous vegetation of mainly short grasses (Fig. 9) and a moderately diverse insect soil fauna composed of solitary bee larvae, soil beetles and their pupae, cicada nymphs, myriapods and other soil insects, as well as oligochaete annelids. Towards the uppermost part of this stage paleosols appear more sporadically than in the lower part of S3 (Fig. 9). Consequently, the uppermost part of the S3 indicates the existence of fluvial floodplain settings that suffered very short to short pauses in deposition, and that —under moderately- to moderately well-drained soil conditions— led to the formation of sporadic incipient soils that supported grassy vegetation (Fig. 9).

Landscape evolution of the Santa Cruz Formation: The reconstructed landscape evolution of the SCF (from S1 to S3; Fig. 9) evidences a continuously aggrading fluvial system that allowed the development of only very poorly- to moderately-developed soils in the floodplain areas. The general absence of well-defined pedofeatures in the paleosols of the middle and upper part of the unit (~ 17.0 to 15.9 Ma) means that this interval was characterized by rapid deposition (*e.g.*, Kraus *et al.*, 2015; Raigemborn *et al.*, 2018b). Thus, it is probable that the progress in pedogenic processes that formed these soils was inhibited by the generally rapidly aggrading conditions of the fluvial system and by the relatively high sedimentation rate (~ 150 m My^{-1} on average) that characterized the SCF (*e.g.*, Perkins *et al.*, 2012; Raigemborn *et al.*, 2015; Cuitiño *et al.*, 2016b; Zapata, 2018; Raigemborn *et al.*, 2018a). In this sense, Daniels (2003) indicated that if floodplain aggradation rate is faster than 0.5 cm yr, recognized soils do not develop.

Although the vertically stacked paleosols of the SCF show a slight reduction in degree of development up-section, this general trend is interrupted by periods with more developed pedogenic features (P3 in S2). This suggests intervals of relatively slower sedimentation and aggradation rates with greater temporal stability. Thus, the greater degree of pedogenesis of P3 compared to P1a, P1b, and P2 of the other stages could be attributed to increased temporal stability due to a more distal position from the active fluvial channels, which allowed pedogenesis and the formation of relatively longer-term stable surfaces. It is also probable that the better development of P3 could be linked to higher moisture conditions (in a context of seasonality in water availability) and consequently, more vegetation cover during its formation. Probably P3 could not progress more in its development due to the existence of a relatively high water table. Finally, the gradual reduction in the pedogenic degree (S3), and the increase

Figure 9. Schematic reconstruction of the landscape evolution in the Santa Cruz Formation (from Stage 1 to Stage 3) including sedimentology, paleosols, plant types (interpreted from phytoliths), and vertebrates (silhouettes). Soil fauna (interpreted from ichnology) is not show. ELCM: Estancia La Costa Member; ELAM: Estancia La Angelina Member; SR: sedimentation rate; PR: pedogenesis rate.

in non-pedogenically modified beds up-section (uppermost part of S3) suggest a progressive increase in sedimentation/aggradation rate of the floodplain. This situation reduced the number and the duration of pauses in deposition, and this impeded the progress in pedogenesis. This trend was probably a consequence of a more continuous pyroclastic input and a less favorable climatic context (*i.e.*, drier conditions than at S2) that could have conditioned the vegetation cover and the soil fauna (Zapata, 2018).

CONCLUSIONS

The middle and upper parts (~ 17.0 to 15.9 Ma) of the Santa Cruz Formation in southernmost Patagonia represent a fluvial system dominated by both epiclastic and pyroclastic distal floodplain deposits that contain different stacked paleosols. These are interpreted as similar to modern Entisols (P1a), Inceptisols (P1b), calcic Inceptisols (P2), and Vertisols (P3) that preserve ichnofossils, and fossil flora and vertebrates. The conjunction of abiotic and biotic data of the analyzed successions of the SCF provides multidisciplinary paleoenvironmental interpretations that allow to reconstruct three different terrestrial landscapes.

The first landscape (middle part of the SCF; upper Estancia La Costa Member) represents an epiclastic distal floodplain bearing weakly developed paleosols (P2). These paleosols supported a mixed environment (open areas with patches of trees) in which a diverse, mixed Santacrucian fauna and a scarce soil fauna developed under relatively warm and seasonally humid conditions. Soil conditions were well-drained with fluctuating soil moisture. P2 formed during short time spans (10^2–10^3 yr) of insignificant or null sedimentation rate and it represents a relatively high sedimentation/pedogenesis ratio in a relatively continuous aggrading environment.

The second reconstructed landscape (the bottom of the lowermost upper part of the SCF; lower Estancia La Angelina Member) is composed of mainly epiclastic distal floodplain settings with minor pyroclastic proximal areas that contain mainly weakly–mildly developed soils (P3). This landscape supported Vertisols and an ecosystem dominated by grasses and palms adapted to variable conditions in hydric availability (C_4 plants), and a soil mesofauna that characterize moderately well-drained soil conditions with a seasonal relatively high water table. Moderately-long (10^3 yr) intervals of landscape stability with low sedimentation/pedogenesis ratio in a more distal position of the floodplain, and relatively warm and seasonal humid conditions —with higher moisture conditions— took place to P3.

Finally, the third landscape (upper part of the SCF; upper Estancia La Angelina Member) attests to the existence of an epiclastic and pyroclastic distal and proximal floodplain over which Protosols with a microthermic (C_3 plants) herbaceous vegetation, and a soil mesofauna formed under moderately well-drained and moderately-drained soil conditions. P1a and P1b developed during very short–short periods of pedogenesis (10^1–10^3 yr) with high ratios of sedimentation/pedogenesis, under a relatively warm and seasonal humid climate, slightly more humid or less seasonal that the climate inferred for the first landscape. Towards the end of the unit, sporadically Protosols developed (P1a and P1b). Although these paleosols represent environmental and ecological conditions similar to those of the lower part of this landscape, a reduction in the number and duration of pauses in deposition, a more continuous volcaniclastic input, and relatively drier conditions characterized the last part of this landscape.

The succession of these different paleolandscapes took place under fluctuating environmental and climatic conditions, in the context of a highly aggrading fluvial system, under relatively warm and humid conditions with variable water availability. The rate of sediment supply, the input of pyroclastic materials, the position on the floodplain, the duration of landscape stability (*i.e.*, pedogenesis time), the alternations of wetter and drier climate phases, and the changes in local hydrologic conditions controlled the soil mesofauna, the vegetation cover, the pedogenic processes, the types of soils, and the degree of soil development.

Acknowledgments

Financial and logistical support for these studies was provided by the projects PIP 100523 of the CONICET (to MSR), and NSF BCS-1749307 (to JMGP). The suggestions made by the reviewers P. Bouza and E. Bedatou, and by the Invited Editor J.I. Cuitiño, greatly improved the quality of this manuscript. The authors would like to thank S. Matheos (CONICET, Argentina), R. Kay (Duke University, USA), M.S. Bargo (CIC, Argentina) and S. Vizcaíno

(CONICET, Argentina) for financial and logistical support, and A. Larroca (UNLP, Argentina), and J. Zuazo and N. Muñoz (CONICET, Argentina) for their assistance during field trips.

REFERENCES

Alonso-Zarza, A.M., and **V.P. Wright**, 2010. Calcretes. In: A.M. Alonso-Zarza and L.H. Tanner (Eds.), *Carbonates in Continental Settings: Facies, Environments and Processes*. Elsevier, Amsterdam, 225-267.

Alonso-Zarza, A.M., M.E., Sanz, J.P.,Calvo, and **P. Estévez**, 1998. Calcified root cells in Miocene pedogenic carbonates of the Madrid Basin: evidence for the origin of Microcodium b. *Sedimentary Geology* 16:81-97.

Ashley, G., and **S. Driese** , 2000. Paleopedology and paleohydrology of a volcaniclastic paleosol interval: implications for Early Pleistocene stratigraphy and paleoclimate record, Olduvai Gorge, Tanzania. *Journal of Sedimentary Research* 70:1065-1080.

Badawy, H.S., 2017. Termite nests, rhizoliths and pedotypes of the Oligocene fluviomarine rock sequence in northern Egypt: Proxies for Tethyan tropical palaeoclimates. *Palaeogeography, Palaeoclimatology, Palaeoecology* 492:161-176.

Barboni, D., and **L. Bremond**, 2009. Phytoliths of East African grasses: An assessment of their environmental and taxonomic significance based on floristic data. *Review of Palaeobotany and Palynology* 158:29-41.

Bargo, M.S., N., Toledo, and **S.F. Vizcaíno** , 2012. Paleobiology of the Santacrucian sloths and anteaters (Xenarthra, Pilosa). In: Vizcaíno, S.F., Kay, R.F. and M.S. Bargo (Eds.), *Early Miocene Paleobiology in Patagonia: high-latitude paleocommunities of the Santa Cruz Formation*. Cambridge University Press, Cambridge, UK, 216-242.

Bellosi, E.S., and **M.G. González**, 2010. Paleosols of the middle Cenozoic Sarmiento Formation, central Patagonia. In: Madden, R.H., Carlini, A.A., Vucetich, M.G., and R.F. Kay (Eds.). *The Paleontology of Gran Barranca: Evolution and Environmental Change through the Middle Cenozoic of Patagonia*. Cambridge University Press, Cambridge, UK, 293-305.

Bertels, A., 1970. Sobre el "Piso Patagoniano" y la representación de la época del Oligoceno en Patagonia Austral, República Argentina. *Revista de la Asociación Geológica Argentina* 25: 496-501.

Biddle, K., M., Uliana R. Jr.,Mitchum, M., Fitzgerald, and **R. Wright**, 1986. The stratigraphic and structural evolution of central and eastern Magallanes Basin, Southern America. In: P. Allen and P. Homewood (Eds), *Foreland basins*. International Association of Sedimentologist, Special Publication 8:41-61.

Billings, E., 1862. New species of fossils from different parts of the Lower, Middle and Upper Silurian rocks of Canada. In: Palaeozoic Fossils (Vol. 1, 1861-1865). *Geological Survey of Canada Advance Sheets*. Canadá, 96-168.

Birkeland, P., 1999. *Soils and geomorphology*. Oxford University Press, New York, 430 pp.

Bradshaw, M.A., 1981. Palaeoenvironmental interpretations and systematics of Devonian trace fossils from the Taylor Group (Lower Beacon Supergroup), Antarctica. *New Zealand Journal of Geology and Geophysics* 24:615-652.

Brea, M., A.F., Zucol, and **A. Iglesias**, 2012. Fossil plant studies from late early Miocene of the Santa Cruz Formation: paleoecology and paleoclimatology at the passive margin of Patagonia, Argentina. In: Vizcaíno, S.F., Kay, R.F. and M.S. Bargo (Eds.), *Early Miocene Paleobiology in Patagonia: high-latitude paleocommunities of the Santa Cruz Formation*. Cambridge University Press, Cambridge, UK, 104-128.

Brea, M., A.F., Zucol, M.S.,Bargo, J.C., Fernícola, and **S.F. Vizcaíno**, 2017. First Miocene record of Akaniaceae in Patagonia (Argentina): a fossil wood from the Early Miocene Santa Cruz Formation and its palaeobiogeographical implications. *Botanical Journal of the Linnean Society* 183:334-347.

Bromley, R.G., 1996. *Trace Fossils: Biology, Taphonomy and Applications*. 2nd Edition, Champman and Hall, London, United Kingdom, 361 pp.

Bullock, P., N., Fedoroff, A., Jongerius, G., Stoops, and **T. Tursina**, 1985. *Handbook for soil thin section description*. Waine Research Publications, 152 pp.

Buol, W.S., R.J., Southard, R.C., Graham, and **P.A. McDanield**, 2011. *Soil genesis and classifications*. 6th Edition, Wiley-Blackwell, Oxford, 543 pp.

Candela, A.M., and **M.B.J. Picasso**, 2008. Functional anatomy of the limbs of Erethizontidae (Rodentia, Caviomorpha): indicators of locomotor behaviour in Miocene porcupines. *Journal of Morphology* 269:552-593.

Candela, A.M., L.L., Rasia, and **M.E. Pérez**, 2012. Paleobiology of Santacrucian Caviomorph rodents: a morpho-functional approach. In: Vizcaíno, S.F., Kay, R.F. and M.S. Bargo (Eds.), *Early Miocene Paleobiology in Patagonia: high-latitude paleocommunities of the Santa Cruz Formation*. Cambridge University Press, Cambridge, UK, 287-305.

Cassini, G.H., 2013. Skull geometric morphometrics and Paleoecology of Santacrucian (late Early Miocene; Patagonia) native ungulates (Astrapotheria, Litopterna, and Notoungulata). *Ameghiniana* 50:193-216.

Catena, A.M., D.I., Hembree, B.Z., Saylor, F., Anaya, and **D.A. Croft**, 2016. Paleoenvironmental analysis of the Neotropical fossil mammal site of Cerdas, Bolivia (middle Miocene) based on ichnofossils and paleopedology. *Palaeogeography, Palaeoclimatology, Palaeoecology* 459:423-439.

Catena, A.M., D.I., Hembree, B.Z., Saylor, F., Anaya, and **D.A. Croft**, 2017. Paleosol and ichnofossil evidence for significant Neotropical hábitat variation during the late middle Miocene (Serravallian). *Palaeogeography, Palaeoclimatology, Palaeoecology* 487:381-398.

Cecil, C.B., and **F.T. Dulong**, 2003. Precipitation models for sediment supply in warm climates. In: Cecil, C.B., and N.T. Edgar (Eds.), *Climate Controls on Stratigraphy*, vol. 77. SEPM Special Publication, 21-27.

Collura, L.V., and **K. Neumann**, 2017. Wood and bark phytoliths of West African woody plants. *Quaternary International* 434 (Part B): 142-159.

Counts, J.W., and **S. Hasiotis**, 2009. Neoichnological experiments with masked chafer beetles (Coleoptera: Scarabaeidae): implications for backfilled continental trace fossils. *Palaios* 24:74-91.

Crifò C., M.S., Bargo, R.F., Kay, M.J., Kohn, S.F., Vicaíno, A.F., Zucol, and **C.A.E. Strömberg**, 2016. Using phytolith to track vegetation changes during the MMCO of the Santa Cruz Formation, Patagonia (Argentina). *XIV International Palynological Congress - X International Organization of Palaeobotany Conference*.

Crifò C., M.S., Bargo, J.I., Cuitiño, R.F., Kay, M.J., Kohn, R.B., Trayler, S.F., Vizcaíno, A.F., Zucol, and **C.A.E. Strömberg**,

2017. Fossil phytolith assemblages from southern Patagonia indicate changing habitats during the Middle Miocene climatic optimum. *GSA Annual Meeting,* Seattle, Washington, USA. DOI: 10.1130/abs/2017AM-298212.

Crifò C., M.S., Bargo, J.I., Cuitiño, R.F., Kay, M.J., Kohn, R.B., Trayler, S.F., Vizcaíno, A.F., Zucol, and **C.A.E. Strömberg**, 2018. Habitat shift during the Middle Miocene Climatic Optimum of Southern Patagonia recorded in phytolith assemblages. *5th International Paleontological Congress* (https://ipc5.sciencesconf.org/).

Cuitiño, J.I., V., Krapovickas, M.S., Raigemborn, L., Zapata, and **J.C. Fernícola**, 2016a. La Formación Monte León (Mioceno temprano) como ejemplo de sistemas sedimentarios transicionales-regresivos de Patagonia Austral. *VII Congreso Latinoamericano de Sedimentología y XV Reunión Argentina de Sedimentología*, 67.

Cuitiño, J.I., J.C., Fernicola, M.J., Kohn, R., Trayler, M.S., Bargo, R.F., Kay, and **S.F. Vizcaíno**, 2016b. U-Pb geochronology of the Santa Cruz Formation (early Miocene) at the Río Bote and Río Santa Cruz (southernmost Patagonia, Argentina): implications for the correlation of fossil vertebrate localities. *Journal of South American Earth Sciences* 70:198-210.

Daniels, J.M., 2003. Floodplain aggradation and pedogenesis in a semiarid environment. *Geomorphology* 56:225-242.

Fanning, D.S., and **M.C.B. Fanning**, 1989. *Soil: Morphology, Genesis, and Classification*. Wiley, 416 pp.

Fidalgo, F., and **J.C. Riggi**, 1970. Consideraciones geomórficas y sedimentológicas sobre los Rodados Patagónicos. *Revista de la Asociación Geológica Argentina* 25:430-443.

Frey, R.W., S.G., Pemberton, and **J. Fagerstrom**, 1984. Morphological, ethological, and environmental significance of the ichnogenera *Scoyenia* and *Ancorichnus*. *Journal of Paleontolology* 58:511-528.

Genise, J.F., 2000. The ichnofamily Celliformidae for Celliforma and allied ichnogenera. *Ichnos* 7:267-282.

Genise, J.F., and **T.M. Bown**, 1994. New Miocene scarabeid and hymenopterous nests and early Miocene (Santacrucian) paleoenvironments, Patagonian Argentina. *Ichnos* 3:107-117.

Genise, J.F., R.N., Melchor, E.S., Bellosi, and **M. Verde**, 2010. Invertebrate and Vertebrate Trace Fossils from Continental Carbonates, In: Alonso-Zarza, A.M., and L.H. Tanner (Eds.), *Developments in Sedimentology*. Elsevier. doi:10.1016/S0070-4571(09)06107-X.

Gile, L.H., F.F., Peterson, and **J.B. Grossman** , 1966. Morphological and genetic sequences of carbonate accumulation in desert soils. *Soil Sciences* 101:347-360.

Halls, J., 1847. *Palaeontology of New York*. Volume I. Containing descriptions of the organic remains of the Lower Division of the New York System (Equivalent to the Lower Silurian rocks of Europe). C. van Benthuysen, Albany, 338 pp.

Harris, E., C., Strömberg, N., Sheldon, S., Smith, and **D. Vilhena**, 2017. Vegetation response during the lead-up to themiddle-Miocene warming event in the Northern Rocky Mountains, USA. *Palaeogeogrraphy, Palaeoclimatology, Palaeoecology* 485:401-415.

Hasiotis, S.T., and **B.F. Platt**, 2012. Exploring the sedimentary, pedogenic, and hydrologic factors that control the occurrence and role of bioturbation in soil formation and horizonation in continental deposits: An integrative approach. *The Sedimentary Record* 4-9.

Hasiotis, S.T., B.F., Platt, D.I., Hembree, and **M.J. Everhart**, 2007. The trace-fossil record of vertebrates. In: Miller, W.I.I.I. (Ed.), *Trace Fossils: Concepts, Problems, Prospects*. Elsevier, 196-216.

Hatcher, J.B., 1897. The cape fair weather beds: a new marine tertiary horizon in southern Patagonia. *American Journal of Science* 4 (IV): 246-256.

Hembree, D.I., and **S.T. Hasiotis**, 2007. Paleosols and Ichnofossils of the White River Formation of Colorado: Insight Into Soil Ecosystems of the North American Midcontinent During the Eocene-Oligocene Transition. *Palaios* 22:123-142.

Hembree, D.I., and **J.J. Bowen**, 2017. Paleosols and ichnofossils of the upper Pennsylvanian lower Permian Monongahela and Dunkard groups (Ohio, USA): a multi-proxy approach to unraveling complex variability in ancient terrestrial landscapes. *Palaios* 32:295-320.

Johnston, P.A., D.A., Eberth, and **P.K. Anderson**, 1996. Alleged vertebrate eggs from upper Cretaceous redbeds, Gobi Desert, are fossil insect (Coleoptera) pupal chambers: Fictovichnus new ichnogenus. *Can. J. Earth Sci.* 33:511-525.

Kay, R.F., S.F., Vizcaíno, M.S., Bargo, J.M.G., Perry, F.J., Prevosti, and **J.C. Fernicola**, 2008. Two new fossil vertebrate localities in the Santa Cruz Formation (late Early-early Middle Miocene, Argentina), 51° South latitude. Journal of South American Earth Sciences 25:187-195.

Kay, R.F., S.F., Vizcaíno, and **M.S. Bargo**, 2012. A review of the paleoenvironment and paleoecology of the Miocene Santa Cruz Formation. In: Vizcaíno, S.F., R.F., Kay and M.S. Bargo (Eds.), *Early Miocene Paleobiology in Patagonia: high-latitude paleocommunities of the Santa Cruz Formation*. Cambridge University Press, Cambridge, UK, 331-365.

Klappa, C.F., 1980. Rhizoliths in terrestrial carbonates: classification, recognition, genesis and significance. *Sedimentology* 27:613-629.

Kohn, M.J., C.A.E., Strömberg, R.H., Madden, R.E., Dunn, S., Evans, A., Palacios, and **A.A. Carlini**, 2015. Quasi-static Eocene–Oligocene climate in Patagonia promotes slow faunal evolution and mid-Cenozoic global cooling. *Palaeogeography, Palaeoclimatology, Palaeoecology* 435:24-37.

Krapovickas, V., 2012. Ichnology of distal overbank deposits of the Santa Cruz Formation (late Early Miocene): paleohydrologic and paleodimatic significance. In: Vizcaíno, S.F., Kay, R.F. and M.S. Bargo (Eds.), *Early Miocene Paleobiology in Patagonia: high-latitude paleocommunities of the Santa Cruz Formation*. Cambridge University Press, Cambridge, UK, 91-103.

Krapovickas, V., M.G., Mángano, **A., Mancuso, C.A., Marsicano,** and **W. Volkheimer**, 2008. Icnofaunas triásicas en abanicos aluviales distales: evidencias de la Formación Cerro Puntudo, Cuenca Cuyana, Argentina. Argentina. *Ameghiniana* 45 (2): 463-472.

Krapovickas, V., P.L., Ciccioli, M.G.,Mángano, C.A., Marsicano, and **C.O. Limarino**, 2009. Paleobiological and paleoecological significance of a Miocene Southa merican ichnofauna in anastomosed fluvial deposits. Países Bajos. *Palaeogeography, Palaeoclimatology, Palaeoecology* 284:129-152.

Krapovickas V., M.S, Bargo S.F., Vizcaíno M.S., Raigemborn and **J.C. Fernicola**, 2013. Huellas fósiles de mamíferos de la Formación Santa Cruz (Mioceno Inferior; provincia de Santa Cruz): aspectos tafonómicos. *XXVII Jornadas Argentinas de Paleontología de Vertebrados*, Libro de resúmenes 55.

Kraus, M., 1999. Paleosols in clastic sedimentary rocks. *Earth Sciences Reviews* 47:41-70.

Kraus, M.J., and **S.T. Hasiotis**, 2006. Significance of different modes of rhizolith preservation to interpreting paleoenvironmental and paleohydrologic settings: examples from

Paleogene paleosols, Bighorn basin, Wyoming, USA. *Journal of Sedimentary Research* 76:633-646.

Kraus, M.J., D.T, Woody, J.J., Smith, and **V. Dukic**, 2015. Alluvial response to the Paleocene-Eocene thermal maximum climatic event, Polecat Bench, Wyoming (USA). *Palaeogeography, Palaeoclimatology, Palaeoecology* 435:177-192.

Krause, J.M., T.M., Bown, E.S., Bellosi, and **J.F. Genise**, 2008. Trace fossils of cicadas in the Cenozoic of Central Patagonia, Argentina. *Palaeontology* 51:405-418.

Machette, M.N., 1985. Calcic soils of the southwestern United States. *Geological Society of America, Special Paper* 203:1-21.

Mack, G.H., W.C., James, and **H.C. Monger**, 1993. Classification of paleosols. *Geological Society of America Bulletin* 105:129–136.

Malumián, N., 1999. La sedimentación y el volcanismo terciarios en la Patagonia Extraandina, 1. La sedimentación en la Patagonia Extraandina. In: R. Caminos (Ed.), *Geología Argentina*. Anales 29 del Instituto de Geología y Recursos Minerales, 557-578.

Matheos, S.D., and **M.S. Raigemborn**, 2012. Sedimentology and paleoenvironment of the Santa Cruz Formation. In: Vizcaíno, S.F., Kay, R.F. and M.S. Bargo (Eds.), *Early Miocene Paleobiology in Patagonia: high-latitude paleocommunities of the Santa Cruz Formation*. Cambridge University Press, Cambridge, UK, 59-82.

Mercader, J., T., Bennett, C., Esselmont, S., Simpson, and **D. Walde**, 2009. Phytoliths in woody plants from the Miombo woodlands of Mozambique. *Annals of Botany* 104:91-113.

Mercader, J., F., Astudillo, M., Barkworth, T., Bennett, C., Esselmont, R., Kinyanjui, D.L., Grossman, S., Simpson, and **D. Walde** , 2010. Poaceae phytoliths from the Niassa Rift, Mozambique. *Journal of Archaeological Science* 37:1953-1967.

Munsell Soil Color Book, 2013. Grand Rapids: Munsell Color: X-Rite, 2013, USA.

Neumann, K., A.G., Fahmy, N., Müller-Scheeßel, and **M. Schmidt**, 2017. Taxonomic, ecological and palaeoecological significance of leaf phytoliths in West African grasses. *Quaternary International* 434 (B): 15-32.

Parras, A. and **J.I., Cuitiño**, (in press). The stratigraphic and paleoenvironmental significance of the regressive Monte Observación Member, Early Miocene of the Austral Basin, Patagonia. *Latin American Journal of Sedimentology and Basin Analysis*.

Pemberton, S.G., and **R.W. Frey**, 1982. Trace fossil nomenclature and the *Planolites Palaeophycus* dilemma. *Journal of Paleontology* 56:843-881.

Perkins, M.E., J.G., Fleagle, M.T., Heizler, B., Nash, T.M., Bown, A.A., Tauber, and **M.T., Dozo**, 2012. Tephrochronology of the Miocene Santa Cruz and Pinturas Formations, Argentina. In: Vizcaíno, S.F., R.F., Kay, and M.S. Bargo (Eds.), *Early Miocene Paleobiology in Patagonia: high-latitude paleocommunities of the Santa Cruz Formation*. Cambridge University Press, Cambridge, UK, 23-40.

Perry, J.M.G., R.F., Kay, S.F., Vizcaíno, and **M.S. Bargo**, 2014. Oldest known cranium of a juvenile New World monkey (Early Miocene, Patagonia, Argentina): implications for the taxonomy and the molar eruption pattern of early platyrrhines. *Journal of Human Evolution* 74:67-81.

PiPujol, M.D., and **P. Buurman**, 1994. The distinction between ground-water gley and surface-water gley phenomena in Tertiary paleosols of the Ebro basin, NE Spain: *Palaeogeography, Palaeoclimatology, Palaeoecology* 110:103-113.

Raigemborn, M.S., L., Gómez-Peral, **J.M., Krause,** and **S.D. Matheos**, 2014. Controls on clay mineral assemblages in an Early Paleogene nonmarine succession: Implications for the volcanic and paleoclimatic record of extra-Andean Patagonia, Argentina. *Journal of South American Earth Sciences* 52:1-23.

Raigemborn, M.S., S.D., Matheos, V., Krapovickas, S.F., Vizcaíno, M.S., Bargo, R.F., Kay, J.C., Fernicola, and **L. Z.apata**, 2015. Paleoenvironmental reconstruction of the coastal Monte Léon and Santa Cruz formations (early Miocene) at Rincón del Buque, southem Patagonia: a revisited locality. *Journal of South American Earth Sciences* 60:31-55.

Raigemborn, M.S., V., Krapovickas, E., Beilinson, L.E., Gómez Peral, **A.F., Zucol, L. F., Zapata, M.R., Kay., M.S., Bargo, S.F., Vizcaíno,** and **A.N. Sial**, 2018a. Multiproxy studies of Early Miocene pedogenic calcretes in the Santa Cruz Formation of southern Patagonia, Argentina indicate the existence of a temperate warm vegetation adapted to a fluctuating water table. *Palaeogeography, Palaeoclimatology, Palaeoecology* 500:1-23.

Raigemborn, M.S., E., Beilinson, J.M., Krause, A.N., Varela, E., Bellosi, S., Matheos, and **N. Sosa** 2018b. Paleolandscape reconstruction and interplay of controlling factors of an Eocene pedogenically-modified distal volcaniclastic succession in Patagonia. *Journal of South American Earth Sciences* 86:475-496.

Ratcliffe, B.C., and **J. Fagerstrom**, 1980. Invertebrate lebensspuren of Holocene floodplains: their morphology, origin and paleoecological significance. *Journal of Paleontology* 54:614-630.

Retallack, G.J., 2001. *Soils of the past*, 2nd Ed. Blackwell Science Ltd., Oxford, 404 pp.

Retallack, G., E., Bestland, and **T. Fremd**, 2000. Eocene and Oligocene paleosols of Central Oregon. *Geological Society of America, Special Paper* 344:1-192.

Sacristán-Horcajada, S., M.E., Arribas, and **R. Mas**, 2016. Pedogenetic calcretes in early Synrift alluvial systems (Upper Jurassic, West Cameros Basin), northern Spain. *Journal of Sedimentary Research* 86:268-286.

Schoeneberger, P.J., D.A., Wysocki, and **E.C. Benham** (Soil Survey Staff), 2012. *Field book for describing and sampling soils*, Version 3.0. Natural Resources Conservation Service, National Soil Survey Center, Lincoln, NE. 300 pp.

Schwertmann, U., and **R.M. Taylor**, 1977. Iron oxides. In J. B. Dixon and S. B Weed (Eds.), *Minerals in Soil Environments*, Madison, Wisconsin: *American Society of Agronomy and Soil Science*, 145-180.

Sheldon, N.D., and **N.J. Tabor**, 2009. Quantitative paleoenvironmental and paleoclimatic reconstruction using paleosols. *Earth-Science Review* 95:1-52.

Soil Survey Staff, 1999. *Soil Taxonomy, a basic system for making and interpreting soil surveys*. United States Department of Agriculture, Handbook, Washington, 436 pp.

Stoops, G., 2003. Guidelines for analysis and description of soil and regolith thin sections: Madison, Wisconsin, *Soil Science Society of America*, 184 pp.

Stoops, G., V., Marcelino, and **F. Mees**, 2010. *Interpretation of micromorphological features of soils and regoliths*. Elsevier, Amsterdam, 720 pp.

Strömberg, C.A.E., R.E., Dunn, R.H., Madden, M.J., Kohn, and **A.A. Carlini**, 2013. Decoupling the spread of grasslands from the evolution of grazer–type herbivores in South America. *Nature Communications* 4: 1478.

Tauber, A.A., 1994. *Estratigrafía y vertebrados fósiles de la Formación Santa Cruz (Mioceno Inferior) de la costa atlántica entre las rías del Coyle y de Río Gallegos, Provincia de Santa Cruz*.

[Ph.D. thesis] Universidad Nacional de Córdoba, República Argentina, 422 pp.

Tauber, A.A., 1997a. Bioestratigrafía de la Formación Santa Cruz (Mioceno inferior) en el extremo sudeste de la Patagonia. *Ameghiniana* 34:413-426.

Tauber, A.A., 1997b. Paleoecología de la Formación Santa Cruz (Mioceno inferior) en el extremo sudeste de la Patagonia. *Ameghiniana* 34:517-529.

Tauber, A.A., R.F., Kay, and **C. Luna**, 2004. Killik Aike Norte, una localidad clásica de la Formación Santa Cruz (Mioceno temprano-medio), Patagonia, Argentina. *Ameghiniana* 41:63-64R.

Tejedor M.F., A.A., Tauber A.L., Rosenberg C.C., Wisher and **M.E. Palacios**, 2006. New primate genus from the Miocene of Argentina. *Proceedings of the National Academy of Sciences of the United States of America,* 103:5437-5441.

Toledo, N., 2016. Conceptual and methodological approaches for a paleobiological integration: the Santacrucian sloths (early Miocene of Patagonia) as a study case. *Ameghiniana* 53:100-141.

Vizcaíno, S.F., M.S., Bargo, R.F., Kay, R.A., Fariña, M., Di Giacomo, M.G., Perry, F.J., Prevosti, N., Toledo, G.H., Cassini, and **J.C. Fernicola**, 2010. A baseline paleoecological study for the Santa Cruz Formation (late-Early Miocene) at the Atlantic coast of Patagonia, Argentina. *Palaeogeography, Palaeoclimatology, Palaeocology* 292:507-519.

Vizcaíno, S.F., R.F., Kay, and **M.S. Bargo**, 2012. *Early Miocene Paleobiology in Patagonia: Highlatitude Paleocommunities of the Santa Cruz Formation*. Cambridge University Press, Cambridge, 370 pp.

Zamanian, K., K., Pustovoytov, and **Y. Kuzyakov**, 2016. Pedogenic carbonates: forms and formation processes. *Earth Science Review* 157:1-17.

Zapata, L., 2018. *Estudio paleoambiental de la Formación Santa Cruz (Mioceno inferior-medio) entre los ríos Coyle y Gallegos, Patagonia Austral, Argentina.* [Ph.D. thesis]. Universidad Nacional de La Plata, La Plata, Argentina, 299 pp.

Zapata, L., V., Krapovickas, M.S., **Raigemborn,** and **S.D. Matheos**, 2016. Bee cell trace fossils associations on paleosols from the Santa Cruz formation: Palaeoenvironmental and palaeobiological implications. *Palaeogeography Palaeoclimatology Palaeoecology* 459:153-169.

Zucol, A.F., E., Passeggi, M., Brea, N.I., Patterer, M.G., Fernández Pepi, and **M.M. Colobig**, 2010. Phytolith analysis for the Potrok Aike Lake Drilling Project: Sample treatment protocols for the PASADO Microfossil Manual. In: H. Corbella and N.I. Maidana (Eds.), *1ª Reunión Internodos del Proyecto Interdisciplinario Patagonia Austral and 1er Workshop Argentino del Proyecto Potrok Aike Maar Lake Sediment Archive Drilling Project*. Proyecto Editorial PIPA. Buenos Aires, Argentina, 81-84.

Zucol, A.F.; M.S., Raigemborn, C.A.E., Strömberg, C., Crifò, E., Passeggi, M.S., Bargo, and **S.F. Vizcaíno**, 2015. Phytolith analysis from Santa Cruz Formation in Rincón del Buque locality (Santa Cruz province, Argentina), Argentina. *XVI Simposio Argentino de Paleobotánica y Palinología*, Libro de Resúmenes: 24-25.

Zucol, A.F., J.M., Krause, M., Brea, M.S., Raigemborn, and **S.D. Matheos**, 2018. Emergence of grassy habitats during the greenhouse–icehouse systems transition in the middle Eocene of central Patagonia. *Ameghiniana* 55:451-482.